Aust. J. Plant Physiol., 1994, **21**, 623–51

Testing a Mechanistic Model of Forest-canopy Mass and Energy Exchange using Eddy Correlation: Carbon Dioxide and Ozone Uptake by a Mixed Oak–Maple Stand

Jeffrey S. Amthor,[A,B] *Michael L. Goulden,*[C] *J. William Munger*[C] *and Steven C. Wofsy*[C]

[A] Woods Hole Research Center, Woods Hole, Massachusetts, USA.
[B] Present address and address for correspondence: Health and Ecological Assessment Division and Global Climate Research Division, L-256, Lawrence Livermore National Laboratory, PO Box 808, Livermore, California 94550-9900, USA; email: Amthor1@LLNL.gov
[C] Division of Applied Sciences and Department of Earth and Planetary Sciences, Harvard University, Cambridge, Massachusetts 02138, USA.

Abstract

A big-leaf model of C_3-canopy mass and energy exchange was used to predict hourly CO_2 and O_3 uptake by a mixed deciduous *Quercus–Acer* (oak–maple) stand in central Massachusetts, USA. The model is based on canopy-radiation interactions, leaf mesophyll metabolism (photosynthetic electron transport, carboxylation and oxygenation of ribulose 1,5-bisphosphate [RuP_2] by RuP_2 carboxylase/oxygenase [Rubisco], and respiration), physical transport conductances of mass and heat above and within the canopy, conductances of mass at the leaf surface and in the mesophyll, and mass and energy exchange at the soil surface (forest floor). Predictions of hourly CO_2 and O_3 uptake were compared to *independent* whole-forest CO_2 and O_3 exchange measurements made by the eddy correlation method during a 68 day period in the summer and early autumn of 1992. Predicted hourly CO_2 exchange rate was strongly correlated ($r \approx +0{\cdot}91$) with measured hourly CO_2 exchange, but mean day-time predicted whole-forest CO_2 uptake was *c.* 13% (*c.* $1{\cdot}13$ μmol CO_2 m^{-2} s^{-1}) greater than CO_2 uptake measured by eddy correlation. The model tended to overpredict CO_2 uptake during late afternoon, but was accurate during the rest of the day. Predicted and measured O_3 uptake rates also were positively correlated ($r \approx +0{\cdot}76$). The diurnal patterns of predicted and measured O_3 uptake indicated that stomatal conductance (g_s) was accurately predicted during the morning, but in the afternoon the model overpredicted g_s. This pattern was consistent with the overprediction of afternoon CO_2 uptake, and suggested that a feedback inhibition of photosynthesis occurred in the afternoon. This might have been related to source–sink imbalance following several hours of photosynthesis. On the whole, and in spite of the simplifications inherent in the big-leaf representation of the canopy, the model is useful for predicting forest–environment interactions and for interpreting mass and energy exchange measurements.

Introduction

There are many reasons to quantify the exchange of mass and energy between a forest canopy and the atmosphere. For example, forest canopy mass and energy exchanges are key factors in forest growth and ecosystem function (Waring and Schlesinger 1985), forest photosynthesis and net primary production are thought to be large components of the global carbon cycle (Bolin *et al.* 1979), and regional forest canopy physiology may influence weather and hydrology (Shukla *et al.* 1990; Eltahir and Bras 1993). Unfortunately, measurements of forest mass and energy exchange are expensive, difficult, and lengthy, and many desirable experiments on forests are impossible to conduct. As a result, simulation models must play a role in clarifying the significance of canopy physics and physiology to biospheric productivity, boundary layer meteorology, regional and global carbon cycling,

0310-7841/94/050623$05.00

and impacts of global environmental change on forest ecosystems. Moreover, models might be used to extrapolate site measurements that are made of forest mass and energy exchange to regional or global scales.

We are developing dynamic multilevel explanatory models (*sensu* Loomis *et al.* 1979; Penning de Vries 1983) of forest ecosystem mass and energy exchange. One component of our program is the construction and testing of a big-leaf representation of a canopy that simulates leaf physiology and mass, energy, and momentum exchanges. The model is based on underlying physical and biochemical principles so that the simulated forest responds to environmental factors such as solar radiation, air temperature, water vapour pressure, precipitation, and atmospheric CO_2 partial pressure according to present understanding of mechanisms involved. Furthermore, we want the canopy model to be simple enough to be dependent on only a small number of input data and parameters, because our long-term goal is the application of the model to regional biospheric CO_2 exchange with the atmosphere in order to: (1) assess present CO_2 source and sink activity of the biosphere, and (2) predict effects of elevated atmospheric CO_2 and other environmental changes on regional ecosystem processes.

The accuracy of a forest physiology model should be tested before it is used to explain or predict forest–atmosphere mass and energy exchange. In order for model tests to be valid, model development and model testing must be separate processes involving independent data. We advocate a four-step procedure for canopy physiology model development and testing, an approach similar to that outlined by Norman (1989):

(1) The model should be developed from 'first principles' and take into account all the factors thought to be quantitatively important. The first principles chosen will depend on the temporal and spatial scales of the model, and in this case include environmental physics (*sensu* Monteith 1973) and leaf biochemistry and physiology (*sensu* Farquhar 1989).
(2) The model should be parameterised for a given site with values for variables such as leaf area index, leaf reflectance, and canopy nitrogen content, but without knowledge of mass or energy exchange. That is, the opportunity for model 'tuning' with site measurements of mass and energy exchange should be avoided.
(3) Model predictions of canopy mass and energy exchange should be made using environmental conditions measured at the test site. In this project we used a 1 h time step to capture the diurnal course of environmental conditions and behaviour of canopy physiology (Grace 1991).
(4) Model predictions should be compared to measurements of mass and energy exchange at the test site that correspond temporally with the environmental data used to drive the model in step (3).

The more often a model is tested, the more confidence can be attached to its predictions. Regrettably, limited availability of direct measurements of forest mass and energy exchange has generally prevented adequate testing of models of forest physiology. The best widely available method for measuring canopy or ecosystem mass and energy exchange, and therefore testing canopy or community physiology models, is eddy correlation. Eddy correlation is a micrometeorological technique, first applied by Swinbank (1951), that measures the net exchange of an entity above an ecosystem with approximately $\pm 20\%$ accuracy over areas extending several tens to hundreds of meters upwind of the instrument tower (Brutsaert 1982; Baldocchi *et al.* 1988; Dabberdt *et al.* 1993). Eddy correlation measurements of ecosystem CO_2 exchange have generally been confined to short periods, i.e. hours to days, which has made it difficult to use those measurements to test models over a broad range of conditions. Indeed, the few tests of models of canopy or ecosystem CO_2 exchange that have been conducted with field data at a temporal resolution of 1 h or less (e.g. Sinclair *et al.* 1976; Baldocchi *et al.* 1987; Norman and Polley 1989; Baldocchi 1993) have generally covered periods of only a few hours to a few days.

To address the need for long-term measurements of ecosystem mass and energy exchange, a multi-year continuous eddy correlation measurement program was initiated in 1990 above a 50- to 70-year-old mixed deciduous midlatitude forest in Massachusetts, USA (Wofsy *et al.* 1993). These data afford the opportunity to test models of forest physiology over long time scales that include a wide range of environmental conditions arising normally during the course of several years. In this paper, we compare predictions of hourly forest CO_2 and O_3 exchange made by our big-leaf canopy physiology model to eddy correlation measurements made during a 68 day period in summer and early autumn of 1992. These comparisons were conducted to: (1) identify model weaknesses and aid in further model development, (2) help in the interpretation of the field measurements, and (3) evaluate effects of the simplifications made in the big-leaf model on the accuracy of its predictions.

Eddy Correlation Method Measurements of Forest CO_2 and O_3 Exchange

Nearly continuous eddy correlation measurements of whole-forest exchanges of CO_2, O_3, sensible heat, latent heat, and momentum have been ongoing in Harvard Forest (42·54°N, 72·18°W; 340 m elevation) since April 1990 (Wofsy *et al.* 1993). A 30 m tower (Rohn 25G) was instrumented with a 3-dimensional sonic anemometer to determine the component wind velocities at the reference height z (30 m above ground, 6–8 m above the canopy). Air was sampled from nearby inlets at height z to measure CO_2 and water vapour by infrared absorption and O_3 by ethylene chemiluminescence. Measurements were recorded at 4 Hz and these data were logged to disk for subsequent analysis. While a faster rate of data collection may be required close to smooth surfaces such as dense crops which lead to smaller eddies, we found that the majority of flux at height z above the rough Harvard Forest is carried by eddies with frequency 0·001–1·0 Hz.

Eddy flux at height z was calculated as the time average of the product of vertical wind speed (w') and the scalar of interest, allowing for the observed time lag to account for the delay in drawing air from height z to the gas analysers on the ground (Wofsy *et al.* 1993). This flux was then corrected for the orientation of the streamlines by rotating the flux tensor to the plane where $\overline{w}' = 0$ (McMillen 1988). A series of simulations, laboratory tests, and spectral analyses have indicated a small loss of flux (< 10%) due to our reliance on closed path detectors. We corrected for this error by scaling the measured CO_2 flux by the ratio of the measured raw heat flux to a heat flux calculated after filtering the temperature signal to simulate an instrument with limited high frequency response (Leuning and King 1992; Wofsy *et al.* 1993). Additional measurements at height z included incident photosynthetic (400–700 nm) photon flux area density (PPFD, mol photons m^{-2} s^{-1})* with a silicon quantum sensor, air temperature (T_a, °C) with an aspirated thermistor, horizontal wind speed ($u(z)$, m s^{-1}) using the sonic anemometer, water vapour pressure (e_a, Pa) using a solid-state probe, ambient CO_2 partial pressure (C_a, Pa) by infrared absorption, and ambient O_3 partial pressure (O_a, Pa) by ultraviolet absorption. Soil surface (forest floor) temperature (T_s, °C) was measured with thermistors at six sites near the tower base.

Measured fluxes and states were averaged over 1 h periods, and for the purpose of testing the big-leaf canopy physiology model we assumed that these hourly values were accurate. We recognise that this was not the case for eddy correlation measurements in practice, and anticipate both random and systematic errors. Random errors associated with the finite averaging time of a measurement (30 min) limit the accuracy of a single observation to about ±20% (Baldocchi *et al.* 1988). Additional difficulties may occur at night when atmospheric stability allows a significant buildup of CO_2 in the airspace below the sensor

* Abbreviations not listed in Tables 1 or 2 (see below): LAI, leaf area index; NIR, near-infrared radiation (700–3000 nm); PAR, photosynthetically active radiation (400–700 nm); PPFD, photosynthetic photon flux density (400–700 nm); RuP_2, ribulose 1,5-bisphosphate; Rubisco, RuP_2 carboxylase/oxygenase.

array, decoupling the flux through the eddy-plane from biotic activity. This CO_2 may then be flushed by sporadic mixing events, resulting in substantial temporal heterogeneity in the measured flux (e.g. Fitzjarrald and Moore 1990). We tried to correct for this by monitoring the change in storage of CO_2 within the airspace below height z and used this change in combination with the eddy-flux measurements to calculate whole-forest CO_2 exchange rate, i.e. the balance of photosynthesis, plant respiration, and decomposition (Wofsy *et al.* 1993). Nonetheless, spatial heterogeneity of CO_2 storage in the canopy airspace resulted in noisy measurements of nighttime exchange. Further complications occur at night when the fluxes and variances in sensor signal approach the noise level of the measurement. These random errors do not, however, introduce a systematic bias into the observations, and their impacts are substantially reduced by considering large measurement data sets.

A careful assessment indicated that systematic errors due to absolute calibration uncertainty were less than 10%. An additional underestimation of flux of up to 10% may have been caused by instrument response and the spatial separation of the anemometer from the gas sampling inlet at height z.

Big-leaf Canopy Mass and Energy Exchange Model

The model used in this study (which is based on Amthor 1994*a*) calculates CO_2, O_3, water, energy, and momentum exchange between a forest and the atmosphere. It does this by combining equations for leaf mesophyll carbon metabolism with transport equations for the canopy boundary layer, leaf boundary layer, leaf surface, leaf mesophyll, and soil 'surface.' The model calculates steady-state mass and energy exchange for a given set of environmental conditions and biological parameters. It comprises five more or less autonomous components.

(1) A model that calculates solar position from site location, date, and time, i.e. SUNAE (Michalsky 1988), and that predicts global shortwave irradiance from measured PPFD (a model input). Global shortwave irradiance is then partitioned between direct beam and diffuse components according to Erbs *et al.* (1982) and direct beam and diffuse radiation are each divided into photosynthetically active radiation (PAR) and near-infrared radiation (NIR) wave bands based on solar elevation (after Szeicz 1974).

(2) A simple multilayer model of NIR and PAR absorption by the canopy that accounts for individual leaf and forest floor reflectance and absorptance of NIR and PAR (Amthor 1994*a*).

(3) A model of transport conductances in the atmosphere and energy balance of the canopy. Temperature, water vapour pressure, CO_2 pressure, and wind speed within the canopy airspace are also simulated.

(4) A model of C_3 leaf mesophyll carbon metabolism (i.e. photosynthesis, photorespiration, and respiration) based on the models of Farquhar *et al.* (1980) and Collatz *et al.* (1991). Carboxylation and oxygenation of ribulose 1,5-bisphosphate (RuP_2) catalysed by RuP_2 carboxylase/oxygenase (Rubisco) are central to the mesophyll metabolism model. Stomatal conductance, at the canopy scale, is linked to photosynthesis in this component of the model.

(5) A model of O_3 uptake into canopy leaves and its short-term effect on Rubisco activity.

For the purpose of simulating canopy physiology (components 3–5), the canopy is represented by a 'big leaf' (*sensu* Sinclair *et al.* 1976) and the soil by a horizontally uniform slab. Environmental and biological parameters that govern big-leaf physiology are listed and defined in Table 1, variables predicted by the big-leaf portion of the model are defined in Table 2, and the structure of the model is shown in Table 3. Unless otherwise stated, all area-based parameters and variables, i.e. with unit m^{-2}, apply to unit horizontal ground area rather than leaf area.

Table 1. Big-leaf canopy physiology model input parameters

Area based parameters except g_c and $g_{s(min)}$ are on a m^{-2} ground area basis; g_c and $g_{s(min)}$ are on a m^{-2} leaf (one side) basis. Parameter values are those used to test the model with eddy correlation measurements made when the tower footprint was dominated by the *Quercus–Acer* stand to the south-west of the tower. Several inputs to the canopy physiology model are outputs from the canopy–radiation interaction model and the boundary layer condition calculations described in the text

Parameter	Symbol	Units	Value [Q_{10}]	Source
Incident PPFD	θ	mol photons m^{-2} s^{-1}	variable	measurement data
Absorbed (by leaves) shortwave radiation	I_a	W m^{-2}	variable	see text
Absorbed (by leaves) PPFD	θ_a	mol m^{-2} s^{-1}	variable	see text
Leaf clumping factor	c	—	0·7	Amthor 1994*a*
Incident longwave irradiance (from sky)	L_{down}	W m^{-2}	variable	see text
Leaf area index	L	m^2 m^{-2}	3·5	1992 site leaf litter
Roughness length of the forest floor	z_S	m	0·01	conjecture
Canopy height	h	m	24	Wofsy *et al.* 1993
Individual leaf mean drag coefficient	c_d	—	0·15	conjecture (see Thom 1968)
Reference (measurement) height	z	m	30	Wofsy *et al.* 1993
Wind speed at reference height z	$u(z)$	m s^{-1}	variable	measurement data
Atmospheric pressure	P	Pa	100×10^3	site average
Vapour pressure at reference height z	e_a	Pa	variable	measurement data
Air temperature at reference height z	T_a	°C	variable	measurement data
Attenuation coefficient for wind speed in canopy	α_{wind}	—	1·0	Bussinger 1975
Leaf absorptance of longwave radiation	α_l	—	0·96	Brutsaert 1982
Individual leaf characteristic dimension	ℓ	m	0·08	site estimate
Abaxial : adaxial stomatal conductance ratio	s_r	—	100	Jones 1992
Leaf cuticular conductance	g_c	mol H_2O m^{-2} s^{-1}	0·005	Jones 1992
Minimum stomatal conductance	$g_{s(min)}$	mol H_2O m^{-2} s^{-1}	0·008	Jones 1992
Stomatal conductance signal from roots	ξ	—	1·0	see text
Stomatal conductance coefficient	k_{stoma}	mol H_2O Pa CO_2 mol^{-1} CO_2	350×10^3	see text
Temperature to which canopy is 'acclimated'	T_{acc}	°C	25°C	based on prevailing T_a
CO_2 partial pressure at height z	C_a	Pa	variable	measurement data
O_2 partial pressure at height z	pO_2	Pa	0·209 P	ambient air
O_3 partial pressure at height z	O_a	Pa	variable	measurement data
Areal concentration of leaf N	N	mol N m^{-2}	0·483	derived in text
Fraction of leaf N that is in Rubisco	f_{rub}	—	0·077	derived in text
Rubisco CO_2/O_2 specificity at 25°C	τ_{rub}	Pa O_2 Pa^{-1} CO_2	2600 [0·57]	Collatz *et al.* 1991
Rubisco catalytic constant with k_t = unity	k_{cat}	mol CO_2 mol^{-1} site s^{-1}	3·3	Woodrow and Berry 1988
Michaelis-Menten constant of Rubisco for CO_2 at 25°C	K_c	Pa	30 [2·1]	Collatz *et al.* 1991
Inhibition constant for O_2 at 25°C	K_o	Pa	30000 [1·2]	Collatz *et al.* 1991
Leaf maintenance respiration coefficient at T_{acc}	m_r	mol CO_2 mol^{-1} N s^{-1}	$3·0\times10^{-6}$	Ryan 1991
Respiratory cost of phloem loading	l_r	mol CO_2 mol^{-1} sucrose	0·55	Amthor 1994*b*
Leaf translocation rate	L_{load}	mol sucrose m^{-2} s^{-1}	$0·35\times10^{-6}$	conjecture
Leaf growth respiration rate	R_g	mol CO_2 m^{-2} s^{-1}	0·0	leaves mature
Soil surface temperature	T_s	°C	variable	measurement data
Longwave radiation emitted by the soil (forest floor)	L_{soil}	W m^{-2}	variable	see text
Soil respiration (CO_2 efflux) rate	R_{soil}	mol CO_2 m^{-2} s^{-1}	variable	see text
Stem respiration (CO_2 efflux) rate	R_{stem}	mol CO_2 m^{-2} s^{-1}	variable	see text

Table 2. Big-leaf canopy physiology model derived variables

All area based parameters are on a per horizontal ground area basis. This list does not include intermediate variables used in the canopy radiation absorption model

Parameter	Symbol	Units
Longwave radiation absorbed by the canopy	L_a	W m^{-2}
Longwave radiation emitted by the canopy	L_e	W m^{-2}
Zero plane displacement height	d	m
Atmospheric stability	ζ	—
Stability correction parameter for momentum	Ψ_M	—
Stability correction parameter for heat	Ψ_H	—
Roughness length for heat	z_H	m
Roughness length for momentum	z_M	m
Friction velocity	u_*	m s^{-1}
Wind speed outside leaf boundary layer	$u(c)$	m s^{-1}
Atmospheric conductance of heat	g_{aH}	m s^{-1}
Atmospheric conductance of water vapour	g_{aW}	mol H_2O m^{-2} s^{-1}
Conductance of heat from the soil surface to canopy airspace	g_{aS}	m s^{-1}
Leaf boundary layer thickness (one side of leaf)	δ	m
Leaf boundary layer conductance of heat (both sides)	g_{bH}	m s^{-1}
Leaf boundary layer conductance of water vapour (both sides)	g_b	mol H_2O m^{-2} s^{-1}
Stomatal conductance of water vapour (both sides)	g_s	mol H_2O m^{-2} s^{-1}
Conductance of water from inside leaf to canopy airspace	g_w	mol H_2O m^{-2} s^{-1}
Conductance of O_3 from reference height z to leaf interior	g_o	mol O_3 m^{-2} s^{-1}
Mesophyll conductance of CO_2	g_{chl}	mol CO_2 m^{-2} s^{-1}
Canopy airspace vapour pressure	e_c	Pa
Vapour pressure in leaf intercellular spaces	e_ℓ	Pa
Vapour pressure gradient through stomatal pores	Δe	Pa
Water vapour flux through horizontal plane at height z	E	mol H_2O m^{-2} s^{-1}
Water vapour flux at the leaf surface	E_ℓ	mol H_2O m^{-2} s^{-1}
Water vapour flux at the soil surface	E_s	mol H_2O m^{-2} s^{-1}
Sensible heat flux through horizontal plane at height z	H	W m^{-2}
Sensible heat flux at the leaf surface	H_ℓ	W m^{-2}
Sensible heat flux at the soil surface	H_s	W m^{-2}
Canopy airspace air temperature	T_c	°C
Canopy (leaf) temperature	T_ℓ	°C
Momentum flux density	τ	kg m^{-1} s^{-2}
Effect of C_i on R_m	r_c	—
Effect of PPFD on R_m	r_ℓ	—
Temperature coefficient for respiration	r_t	—
Leaf maintenance respiration rate	R_m	mol CO_2 m^{-2} s^{-1}
Leaf respiration rate	R_d	mol CO_2 m^{-2} s^{-1}
Temperature coefficient for photosynthesis	k_t	—
Maximum rate of RuP_2 carboxylation	$V_{c(max)}$	mol CO_2 m^{-2} s^{-1}
CO_2 compensation point with $R_d = 0$	Γ_*	Pa
RuP_2-saturated rate of carboxylation	W_c	mol CO_2 m^{-2} s^{-1}
Fraction of Θ_a that is absorbed by PS I or PS II	f_{PS}	—
Potential rate of whole-chain electron transport	J	mol e^- m^{-2} s^{-1}
Electron-transport-limited rate of carboxylation	W_j	mol CO_2 m^{-2} s^{-1}
Capacity for leaf triose-P use	Φ	mol triose-P m^{-2} s^{-1}
Rate of RuP_2 carboxylation limited by P_i regeneration	W_t	mol CO_2 m^{-2} s^{-1}
Rate of RuP_2 carboxylation in the absence of stress	V_c	mol CO_2 m^{-2} s^{-1}
Photosynthesis (RuP_2 carboxylation) rate	P_s	mol CO_2 m^{-2} s^{-1}
Photorespiration (glycine decarboxylation) rate	P_r	mol CO_2 m^{-2} s^{-1}
Canopy CO_2 assimilation rate	A_{net}	mol CO_2 m^{-2} s^{-1}
Canopy airspace CO_2 partial pressure	C_{can}	Pa
Intercellular CO_2 partial pressure	C_i	Pa
Chloroplast stroma CO_2 partial pressure	C_c	Pa
Rate of O_3 uptake into leaves	F_o	mol O_3 m^{-2} s^{-1}
Relative inhibition of V_c by O_3 uptake	α_{ozone}	—
Flux of CO_2 through the horizontal plane at height z	$F(z)$	mol CO_2 m^{-2} s^{-1}

Table 3. Big-leaf canopy physiology model structure

Read environmental conditions
Call earth–sun geometry, solar radiation partitioning (diffuse/direct), and solar radiation exchange models
Calculate d, z_H, z_M, and other static parameters
Find a value of T_c less than, and a value greater than, steady-state T_c
Do until T_c is stable (using Brent's algorithm[A])
  Find a value of u_* less than, and a value greater than, steady-state u_*
  Do until u_* is stable (using Brent's algorithm[A])
    Calculate ζ, Ψ_H, Ψ_M, and atmospheric, leaf boundary layer, and soil surface conductances
    Calculate soil surface (forest floor) mass and energy exchange rates
    Find a value of e_c less than, and a value greater than, steady-state e_c
    Do until e_c is stable (using Brent's algorithm[A])
      Find a value of C_{can} less than, and a value greater than, steady-state C_{can}
      Do until C_{can} is stable (using Brent's algorithm[A])
        If night-time then
          Set $g_s = g_{s(min)}\ L$
          Find a value of T_ℓ less than, and a value greater than, steady-state T_ℓ
          Do until T_ℓ is stable (using Brent's algorithm[A])
            Calculate leaf (canopy) energy exchange with this T_ℓ and set new value of T_ℓ
          End do
          Find a value of C_i less than, and a value greater than, steady-state C_i
          Do until C_i is stable (using Brent's algorithm[A])
            Calculate R_d (i.e. A_{net}) based on this T_ℓ and C_i
            Calculate C_i based on this A_{net} and C_{can} and set new value of C_i
          End do
        Else if day-time then
          Find a value of g_s less than, and a value greater than, steady-state g_s
          Do until g_s is stable (using Brent's algorithm[A])
            Calculate g_o, F_o, and α_{ozone}
            Find a value of T_ℓ less than, and a value greater than, steady-state T_ℓ
            Do until T_ℓ is stable (using Brent's algorithm[A])
              Calculate leaf (canopy) energy exchange with this T_ℓ and set new value of T_ℓ
            End do
            Find a value of C_c less than, and a value greater than, steady-state C_c
            Do until C_c is stable (using Brent's algorithm[A])
              Calculate P_s, R_d, and A_{net} based on this T_ℓ and C_c
              Calculate C_c and C_i based on this A_{net}, C_{can} and g_s and set new value of C_c
            End do
            Calculate g_s with present variable values and set new value of g_s
          End do
        End if
        Calculate C_{can} with present A_{net} and set new value of C_{can}
      End do
      Calculate e_c with present E_ℓ and set new value of e_c
    End do
  End do
End do
Calculate momentum flux density

[A] The procedure ZERO of Brent (1973, chapter 4) is used.

This big-leaf approach to simulating canopy physiology is based on the hypothesis that the metabolic properties of leaf organelles and cells can be quantitatively mapped onto (scaled up to *sensu* Caldwell *et al.* 1993) whole leaves (see, e.g., Farquhar 1989) and that properties of individual leaves can in turn be mapped onto (scaled up to) canopies (see, e.g., Field 1991; Sellers *et al.* 1992; Amthor 1994*a*). As a result, with respect to CO_2 assimilation, the canopy can be treated as a single big leaf or superleaf; that is, the photosynthetic properties of chloroplasts are assumed to be scaled within leaves according to PPFD absorption profiles within leaves, and similarly, the photosynthetic properties of individual leaves are assumed to be scaled with depth in the canopy in relation to canopy PPFD profiles. Stomatal conductance, PPFD-compensation point, and leaf respiration also are assumed to be scaled with canopy PPFD profiles as discussed by, e.g., Caldwell *et al.* (1986). Because of this, a canopy can behave as a single big leaf that absorbs the same amount of light as the canopy and assimilates CO_2 in accordance with the total photosynthetic machinery present throughout the canopy (Amthor 1994*a*). This scaling is assumed to be an intrinsic property of the canopy itself, resulting from evolutionary selection of canopy species through functional convergence (see Field 1991). The scaling is related to a strong positive relationship between vertical patterns of PPFD and leaf N per unit leaf area, as recently reported for an *Acer saccharum* canopy (Ellsworth and Reich 1993; see also references therein). (*Nota bene*: the 'parallel' vertical gradients of leaf photosynthetic properties and PPFD may not apply to crop canopies during grain filling [e.g. Sandras *et al.* 1993].)

It has been suggested that canopy models should at least divide the leaves into sunlit and shaded fractions, and that a canopy might be also divided into several horizontal layers (see, e.g. Norman 1980, 1993). Multilayer models, or sunlit/shaded big-leaf models, integrate (i.e. sum rather than scale) individual-leaf photosynthesis model predictions for multiple canopy layers, or sunlit and shaded fractions of a big leaf, to arrive at whole-canopy predictions (see Baldocchi 1993; Norman 1993). Sunlit and shaded fractions of the canopy are not, however, distinguished in this model, although canopy radiation absorption is calculated with a multilayer model that distinguishes direct beam from diffuse radiation. That is, this big-leaf model considers the whole canopy as an operational unit analogous to a leaf with respect to mesophyll metabolism for the reasons mentioned above. Justification of this big-leaf approach to modelling canopy photosynthesis and energy exchange have been discussed in Sellers *et al.* (1992) and Amthor (1994*a*). Nonetheless, the model does contain an element of a sunlit/shaded leaf distinction. Namely, the rate of carboxylation V_c is defined by smoothed transitions among the limitations W_c, W_j, and W_t (see Appendix), which we interpret as a colimitation on actual carboxylation by all three capacities. The smoothing implies that different leaves in the canopy will diverge to different degrees from perfect relationships between canopy depth, PPFD, and photosynthetic capacity. The same argument was made by Kirschbaum and Farquhar (1984) with respect to different chloroplasts in models of leaf photosynthesis. Values of the smoothing factors (0·96 and 0·98 in this model, see Appendix) have been empirically set, not derived from first principles. We emphasise that this big-leaf model is not a model of an 'average' leaf with an area equal to LAI. If that were the case a distinction between sunlit and shaded fractions of the canopy would be necessary. Indeed, predicted big-leaf physiological rates differ significantly from rates for individual leaves or average leaves of a species under the same environmental conditions.

Model Parameterisation

The big-leaf canopy model was parameterised whenever possible with values from the literature (see Table 1). The model did not rely on any leaf or canopy CO_2 or O_3 flux measurements made at Harvard Forest, so its predictions were *independent* of site measurements of CO_2 or O_3 fluxes. Estimates of soil and stem CO_2 release rates

(R_{soil} and R_{stem}, respectively, both in mol CO_2 m^{-2} s^{-1}), which are boundary conditions of the canopy model, were based on whole-forest eddy correlation and small chamber measurements at the site (see below).

Differences between this and the previous version (Amthor 1994*a*) of the big-leaf canopy physiology model, and its boundary conditions, are described below. Equations making up the big-leaf canopy physiology component of the forest mass and energy exchange model are given in the Appendix.

Species Composition and Leaf Area of the Forest Stand

Near the eddy correlation tower the forest was a mixture of *Quercus rubra* L., *Acer rubrum* L., *Betula alleghaniensis* Britt., and *Fagus grandifolia* Ehrh., with isolated stands of *Pinus resinosa* Ait. and *Tsuga canadensis* (L.) Carr. to the north-west and east of the tower. When the wind was from the south-west, i.e. between 180° and 270° (magnetic north = 0°), the tower footprint was dominated by *Quercus* (approximately 70% of leaf area) and *Acer* (approximately 30% of leaf area) trees with a total leaf area index (L, m^2 leaf m^{-2} ground) of *c.* 3·5, as determined by leaf litter collected at the site in 1992. The model was applied to the forest to the south-west of the tower and therefore parameterised for a mixture of 70% *Quercus* and 30% *Acer* leaf area. The notation $f_{Quercus}$ (= 0·70) is used to indicate the fraction of canopy leaf area that was *Quercus* and f_{Acer} (= 0·30) is used to indicate the fraction that was *Acer*.

Amount of Rubisco in the Canopy

Key model inputs include the amount of leaf nitrogen in the canopy (N, mol N m^{-2} *ground*), the catalytic constant of Rubisco for RuP_2 carboxylation (k_{cat}, mol CO_2 assimilated mol^{-1} Rubisco catalytic site s^{-1}), and the fraction of N that is in Rubisco (f_{rub}, dimensionless). N can be measured easily at any site and, at a site about 1 km from the eddy correlation tower, *Quercus* and *Acer* leaves contained about 0·15 and 0·11 mol N m^{-2} *leaf*, respectively (Aber *et al.* 1993), so N was set to (0·15 $f_{Quercus}$ + 0·11 f_{Acer}) L or 0·483 mol N m^{-2} *ground* (Table 1).

Values of k_{cat} may be relatively invariant among C_3 species and, since this value has not been determined at Harvard Forest, we set k_{cat} to 3·3 (Woodrow and Berry 1988). In the model this value of k_{cat} applies at the temperature to which canopy leaves are acclimated (T_{acc}, °C). For this model test T_{acc} was set to 25°C. We will discuss the calculation of T_{acc} and its implications for simulating photosynthesis and respiration elsewhere. The value of k_{cat} is related to leaf temperature (T_l, °C) by the temperature coefficient k_t (see Appendix).

Estimates of f_{rub} are also not available for Harvard Forest. We note that f_{rub} can be calculated, with k_t = unity, by rearranging equation A33 (Appendix) as follows

$$f_{rub} = V_{c(max)}/(0{\cdot}00125\ N\ k_{cat}), \quad (1)$$

where $V_{c(max)}$ is the capacity of Rubisco to assimilate CO_2 (mol CO_2 m^{-2} s^{-1}) at T_{acc}, and 0·00125 is the number of Rubisco reaction sites per N atom in a Rubisco molecule. To our knowledge, however, estimates of $V_{c(max)}$ have not been made for forest trees near the eddy correlation tower nor for other large forest trees *in situ*, so equation (1) cannot be solved with data from the site. But, $V_{c(max)}$ has been estimated for individual leaves of several trees, albeit seedlings and saplings, including three *Quercus*, one *Acer*, one *Betula*, one *Fagus*, and two *Pinus* species (derived and summarised in Wullschleger 1993). Those values of $V_{c(max)}$ included 30, 36, and 49 μmol CO_2 m^{-2} *leaf* s^{-1} at 25°C and 18 and 51 μmol CO_2 m^{-2} *leaf* s^{-1} at 30°C for *Quercus*. They also included 19 and 30 μmol CO_2 m^{-2} *leaf* s^{-1} at 25°C for *Acer*. Since we are interested in estimates of stress-free

or potential photosynthetic capacity for use in the model, the higher values of $V_{c(max)}$ tabulated by Wullschleger (1993) for 25°C were used to parameterise the model.

If near the eddy correlation tower *Quercus* leaf $V_{c(max)}$ was 50 μmol CO_2 m^{-2} *leaf* s^{-1} and N was 0·15 mol N m^{-2} *leaf*, the value of f_{rub} would have been *c.* 0·081 with k_t = unity. Similarly, if *Acer* leaf $V_{c(max)}$ at the site was 30 μmol CO_2 m^{-2} *leaf* s^{-1} and N was 0·11 mol N m^{-2} *leaf*, f_{rub} would have been *c.* 0·066 with k_t = unity. By comparison, f_{rub} exceeded 0·3 for well fertilised *Pisum sativum* (Makino and Osmond 1991), and values in the range 0·15–0·30 may be common for other herbaceous plants (Evans 1989).

For model parameterisation, the *Quercus–Acer* stand f_{rub} was set to (from the above)

$$(0{\cdot}081 \times 0{\cdot}7 \times 0{\cdot}15 + 0{\cdot}066 \times 0{\cdot}3 \times 0{\cdot}11)/(0{\cdot}7 \times 0{\cdot}15 + 0{\cdot}3 \times 0{\cdot}11),$$

which is *c.* 0·077 mol N in Rubisco per mol N in the canopy (Table 1). Thus *c.* 80% of the Rubisco in the canopy, and therefore 80% of the photosynthetic capacity of the canopy, was associated with *Quercus* in this parameterisation although only 70% of the leaf area was *Quercus*. This estimate of f_{rub} for a forest stand implies that part of the generally lower photosynthetic capacity of forest tree leaves compared to leaves of many herbaceous species (see Wullschleger 1993) is due to a relatively small fraction of leaf nitrogen being used for photosynthetic enzymes, rather than an inherently limited carboxylation capacity per unit of Rubisco. This point deserves study *in situ* as it may be central to the capacity for CO_2 assimilation by forests.

Stomatal Conductance

It is a matter of contention whether leaf water potential has a direct effect on photosynthesis or affects CO_2 assimilation only through stomatal aperture (see, e.g., Lauer and Boyer 1992). This issue has been discussed with respect to modeling photosynthesis by Friend (1991), who related photosynthesis to leaf water potential directly. In our previous approach (Amthor 1994*a*) we also related RuP_2 carboxylation rate (P_s, mol CO_2 m^{-2} s^{-1}) and stomatal conductance (g_s, mol H_2O m^{-2} s^{-1}) to an estimate of leaf water potential. In the present model, however, g_s is related to the difference in vapour pressure in the substomatal cavity and the outside of the stomatal pores (Δe, Pa) instead of to leaf water potential. Moreover, P_s is independent of leaf water potential and humidity in the model. The value of Δe is given by

$$\Delta e = e_\ell - e_c + E_\ell P/g_b, \qquad \Delta e \geq 0, \tag{2}$$

where e_ℓ is vapour pressure in the leaf intercellular spaces (Pa), e_c is vapour pressure in the canopy airspace (Pa), E_ℓ is big-leaf transpiration rate (mol H_2O m^{-2} s^{-1}), P is atmospheric pressure (Pa), and g_b is conductance of the big-leaf boundary layer (mol H_2O m^{-2} s^{-1}). Saturation vapour pressure at T_ℓ was equated with e_ℓ.

Except for the substitution of a humidity term for the leaf water potential term, g_s is related to P_s as before (Amthor 1994*a*) as follows

$$g_s = \xi[g_{s(min)}L + k_{stoma} \exp(-0{\cdot}00045\ \Delta e)\ P_s/C_i], \tag{3}$$

where ξ is a signal (0–1) from roots pertaining to soil water status that partially controls stomatal conductance (see, e.g., Gollan *et al.* 1986); $g_{s(min)}$ is the minimum stomatal conductance, i.e. the value with closed stomata (mol H_2O m^{-2} *leaf* s^{-1}); k_{stoma} is an empirical coefficient; C_i is the intercellular CO_2 partial pressure (Pa); and exp (x) means e^x.

The form of the response of g_s to Δe is based on, e.g., Mott and Parkhurst (1991) and Aphalo and Jarvis (1993), although it has been suggested that stomata respond to E_ℓ rather than Δe (Grantz 1990; Mott and Parkhurst 1991). The parameter ξ reflects a signal regarding soil water status on the time scale of days, whereas stomatal response to Δe is an instantaneous response to humidity or transpiration rate. A similar set of long-term and instantaneous controls on g_s has been suggested by Tardieu and Davies (1993). For this model test ξ was set to unity (high soil water content) because the soil in the root zone was generally moist during summer and early autumn 1992 (unpublished observations).

A value of 350×10^3 was assigned to the empirical coefficient k_{stoma} (Table 1) because the model then predicted, for high PPFD and normal humidity conditions, values of *c.* 0·65–0·70 for the ratio C_i/C_{can} at the eddy correlation site (C_{can} is the partial pressure of CO_2 in the canopy airspace in Pa). We consider that range of values typical for C_3 leaves. A similar range was predicted by Friend's (1991) model of optimal g_s for individual leaves.

Relationships between photosynthesis and conductance have been discussed by, e.g., Farquhar and Wong (1984) and Lee and Bowling (1992). Use of P_s in equation (3) implicitly incorporates effects of PPFD, N, and T_ℓ on g_s. This approach differs slightly from that of Collatz *et al.* (1991) who used net leaf CO_2 exchange rate A_{net} rather than P_s to calculate g_s. Equation (3) can be applied at any PPFD or photosynthetic rate.

The inverse relationship between g_s and C_i (rather than the CO_2 partial pressure at another location) is based on Mott (1988). It results in a somewhat conservative ratio between C_i and C_{can}.

Ozone Uptake and Inhibition of Photosynthesis by Ozone

Conductance of O_3 from the reference height z to the intercellular spaces (g_o, mol O_3 m^{-2} s^{-1}) is calculated by

$$g_o = 1/(1/g_{aW} + 1{\cdot}41/g_b + 1{\cdot}67/g_s)\,, \tag{4}$$

where g_{aW} is the conductance of water vapour from height z into the canopy airspace (mol H_2O m^{-2} s^{-1}). The term $1/g_{aW}$ implies that atmospheric conductance of O_3 is equal to atmospheric conductance of water vapour because that conductance is based on turbulent transport. The value 1·41 approximates the relative flow of water vapour and O_3 through a laminar leaf boundary layer, i.e. $1{\cdot}41 = 1{\cdot}67^{\frac{2}{3}}$ (Thom 1968), where transport is a combination of diffusion and bulk flow. The value 1·67 is the binary diffusion coefficient of water vapour in air divided by the binary diffusion coefficient of O_3 in air (from Laisk *et al.* 1989).

In the model, the flux of O_3 *into leaves* (F_o, mol O_3 m^{-2} s^{-1}) is given by

$$F_o = g_o O_a/P\,. \tag{5}$$

Equation (5) is based on the assumption that intercellular O_3 partial pressure is zero (Laisk *et al.* 1989).

It is well known that O_3 inhibits photosynthesis, and the model includes a parameter α_{ozone} that denotes the relative inhibition of P_s by O_3 taken up into leaves per unit Rubisco in the canopy

$$\alpha_{ozone} = 0{\cdot}6 \times 10^6\, F_o/(f_{rub}N) \qquad \alpha_{ozone} \leq 1\,. \tag{6}$$

Use of α_{ozone} is shown in Appendix. The coefficient $0{\cdot}6\times10^6$ was derived from results reported by Reich and Amundson (1985) for tree leaves. Note that α_{ozone} is related to

present O_3 uptake rate; it does not account for damage to the photosynthetic machinery that might have resulted from previous (hours to days) exposure of the mesophyll to O_3. Equation (6) is a working hypothesis with respect to the big-leaf physiology model.

Boundary Conditions

Boundary conditions for the big-leaf canopy physiology model include results of the canopy–radiation interaction calculations, environmental variables measured at height z, and mass and energy fluxes at the soil surface and from stems. Calculations of boundary conditions not measured at the site, or described in Amthor (1994*a*), are outlined below.

Longwave Irradiance

Because longwave irradiance (L_{down}, W m^{-2}) is not commonly measured, it is calculated from more frequently measured environmental variables as follows (see Brutsaert 1982)

$$\epsilon_{ac} = [0{\cdot}045\, e_a/(273{\cdot}15 + T_a)]^{\frac{1}{7}} \tag{7}$$

$$c_s = 1{\cdot}1976\, f_{dif} - 0{\cdot}1976 \qquad 0 \leq c_s \leq 1, \quad \text{day-time} \tag{8a}$$

$$c_s = 0{\cdot}25 \qquad \text{night-time} \tag{8b}$$

$$L_{down} = \epsilon_{ac}\, \sigma (273{\cdot}15 + T_a)^4 (1 + a_c\, c_s^2)\,, \tag{9}$$

where ϵ_{ac} is the estimated atmospheric emissivity under clear skies; c_s is the fraction of sky covered by clouds; f_{dif} is the fraction of shortwave irradiance that is diffuse (i.e. not direct beam); and a_c is the Bolz parameter a, which is related to sky conditions and was set to 0·22, which corresponds to 'average' cloudy conditions (Brutsaert 1982). The value of f_{dif} is calculated by model component 1. Cloud cover c_s is set to 0·25 at night as a crude proxy for actual cloud cover because it cannot be calculated from site measurements used in this model test.

Soil and Stem Respiration

Both R_{soil} and R_{stem} are required to calculate C_{can} and therefore photosynthesis. They were derived from measurements of whole-ecosystem respiration rates (R_{forest}, mol CO_2 m^{-2} s^{-1}). Empirical equations for R_{forest} were derived from night-time net ecosystem CO_2 exchange rate and T_s measurements made during well mixed periods (friction velocity $u_* > 0{\cdot}17$ m s^{-1}) throughout 1992. Different equations were developed for different wind directions. When the wind was from the south-west, which applies to the *Quercus–Acer* stand, R_{forest} was given by ($r^2 \approx 0{\cdot}4$ for 1992)

$$R_{forest} = 4 \times 10^{-6} \times 2{\cdot}5^{[(T_s - 20)/10]}\,. \tag{10}$$

Reliance on T_s as the sole driver of R_{forest} was appointed by a series of chamber measurements of soil and bole respiration that established the dominant role of R_{soil} to night-time R_{forest} (Wofsy *et al.* 1993) and the primary role of T_s in determing R_{soil}.

The estimated value of R_{forest} was then used to assign values to R_{soil} and R_{stem} as follows

$$R_{soil} = 0{\cdot}70\, R_{forest} \tag{11}$$

$$R_{stem} = 0{\cdot}10\, R_{forest}\,. \tag{12}$$

Leaf respiration, which according to equations (11) and (12) should be 0·2 R_{forest}, is calculated by the big-leaf canopy physiology model. The present work is not a test of predictions of whole-forest respiration; the values of R_{soil} and R_{stem} are boundary conditions for the canopy model.

Soil Energy Balance and Evaporation

Shortwave radiation reflected up by the forest floor, longwave radiation emitted by the forest floor (L_{soil}, W m^{-2}), sensible heat exchange between the forest floor and the canopy airspace (H_s, W m^{-2}), and soil evaporation rate (E_s, mol H_2O m^{-2} s^{-1}) are boundary conditions of the canopy physiology model. Forest floor shortwave radiation reflection is calculated by model component 2 (described in Amthor 1994*a*).

L_{soil} is given by

$$L_{soil} = \alpha_s \sigma (273{\cdot}15 + T_s)^4 , \tag{13}$$

where α_s is the longwave absorptance of the forest floor (set to 0·96 for this model test) and σ is the Stefan-Boltzmann constant (5·6697×10^{-8} W m^{-2} K^{-4}).

Conductance of heat from the forest floor to the canopy airspace (g_{aS}, m s^{-1}) is adapted from Shuttleworth and Wallace (1985) as follows

$$g_{aS} = \kappa^2 u(z)\, \alpha_{wind}\, (h - d)/(\ln [(z - d)/z_M]h[\exp (\alpha_{wind}) - \exp (\alpha_{wind} [1 - (d + z_M)/h])]) , \tag{14}$$

where κ is von Kármán's constant, taken to be 0·4 (Brutsaert 1982), and the other parameters are defined in Tables 1 and 2.

Sensible heat exchange at the forest floor is given by

$$H_s = c_p \rho g_{aS} (T_s - T_c) , \tag{15}$$

where c_p is the specific heat of air (1012 J kg^{-1} K^{-1}); ρ is the density of air in the canopy airspace, which is a $f(T_c, e_c, P)$; and T_c is the temperature of the air in the canopy airspace (°C).

For present purposes the simple soil evaporation model of Choudhury and Monteith (1988) was used. That model applies to a dry surface soil layer underlaid by a wet subsurface layer from which water evaporates. The depth to wet soil, i.e. the thickness of the upper dry layer (l_d, m), was set to 0·03 m for our simulations, a value not inconsistent with site observations during 1992. The temperature of the interface between the 'wet' and 'dry' soil (T_w, °C) was defined as the mean of T_a and T_s in the present simulations. Changes in values of the parameters l_d and T_w had negligible effects on predictions of the big-leaf model for the eddy correlation site during the test period.

Conductance of water vapour through the dry surface layer (g_{wS}, mol H_2O m^{-2} s^{-1}) is given by

$$g_{wS} = p_{soil} D_{wv} P/(\tau_{soil}\, l_d\, R\, [273{\cdot}15 + (T_s + T_w)/2]) , \tag{16}$$

where p_{soil} is the air-filled porosity of the soil (set to 0·4 for this test); D_{wv} is the diffusion coefficient of water vapour in air, which is a $f(T_s, T_w)$; τ_{soil} is the tortuosity of the soil pore spaces (set to 2); and R is the gas constant (8·3144 J mol^{-1} K^{-1}).

Soil evaporation rate E_s is then given by

$$E_s = (e_w - e_c)/(P/g_{wS} + [R\,(273{\cdot}15 + T_w)/g_{aS}]), \quad (17)$$

where e_w is the saturation vapour pressure (Pa) at T_w.

Prediction–Measurement Comparisons

Predicted whole-ecosystem CO_2 exchange rate is given by the rate of net canopy CO_2 exchange (A_{net}, mol CO_2 m^{-2} s^{-1}) minus (R_{soil}+R_{stem}). A_{net} is positive when photosynthesis exceeds the sum of leaf respiration and photorespiration. R_{soil} and R_{stem} are taken to be positive, although they represent a negative CO_2 flux into the forest.

To test the canopy physiology model, we compared hourly whole-forest eddy correlation measurements of CO_2 and O_3 exchange to model predictions when the wind was from the south-west (i.e. when the tower footprint was dominated by the *Quercus-Acer* stand) during a 68 day period in July, August, and September 1992. We also compared predictions for the *Quercus-Acer* stand to measuremtns for other wind directions to compare *Quercus–Acer* stand fluxes to whole-forest fluxes. Hourly summaries of mean measured mass exchange rates were compared to model predictions of mass exchange rate pertaining to the midpoint of each hour for purposes of solar position calculation. Hourly means of the environmental conditions measured at height z were used as input to the model (see Table 1) although, when environmental conditions are varying rapidly, a shorter time step may be beneficial (Wang *et al.* 1992).

Our goal is to test separately each component of the forest ecosystem mass and energy exchange models we are developing in order to understand the strengths and weaknesses of each component. Such understanding is needed to evaluate predictions of the whole-ecosystem model. The emphasis herein is on day-time forest physiology because a canopy model is being tested rather than the whole ecosystem carbon cycling model. Day-time ecosystem CO_2 fluxes are typically dominated by photosynthesis whereas night-time fluxes are due to plant and soil respiration. Night-time fluxes were nonetheless calculated and compared to measurements, in part to test our estimates of boundary conditions.

Results and Discussion

Hourly CO_2 Exchange

The pooled day-time (i.e. during the period from civil sunrise to civil sunset) hourly *Quercus–Acer* stand CO_2 fluxes measured by eddy correlation and predicted by the model were both hyperbolically related to incident PPFD (Fig. 1*A*, *B*). The eddy correlation measurements did not show a clear PPFD-saturation point, whereas the model predicted PPFD-saturation for the conditions of the study at about 1000 μmol photons m^{-2} s^{-1}, or just over half the maximum hourly PPFD measured during the test period. Both measured and predicted CO_2 uptake were generally slower at a given PPFD in the afternoon than they were in the morning (compare open and filled symbols in Fig. 1), as discussed below. The measured difference between morning and afternoon CO_2 exchange at low PPFD was greater than the predicted difference at low PPFD.

The variation in eddy correlation measurements of CO_2 uptake at a given PPFD was greater than the variation in model predictions (Fig. 1). Related to this, the predicted day-time *Quercus–Acer* CO_2 uptake rates had a smaller range than the measured rates; the predicted day-time rates ranged from *c.* -5 to 20 μmol CO_2 m^{-2} s^{-1} whereas the measured rates ranged from *c.* -10 to 23 μmol CO_2 m^{-2} s^{-1} (Figs 1 and 2). Predicted day-time hourly *Quercus–Acer* CO_2 uptake rate was, however, strongly correlated with the measured hourly CO_2 uptake during the 242 test hours when the wind was from the south-west (product–moment correlation coefficient $r \approx +0{\cdot}91$, $P < 0{\cdot}0001$; Sokal and

Rohlf 1981). The mean measured hourly day-time CO_2 assimilation rate during those test hours was *c.* 8·73 μmol CO_2 m^{-2} s^{-1}. The mean rate predicted by the model for the same hours was *c.* 9·86 μmol CO_2 m^{-2} s^{-1}, which was significantly greater (*c.* 13%) than the measured value according to a *t*-test for paired comparisons ($P < 0{\cdot}0001$, d.f. = 241; Sokal and Rohlf 1981). Many of the model overpredictions of CO_2 uptake rate occurred after noon (Fig. 2).

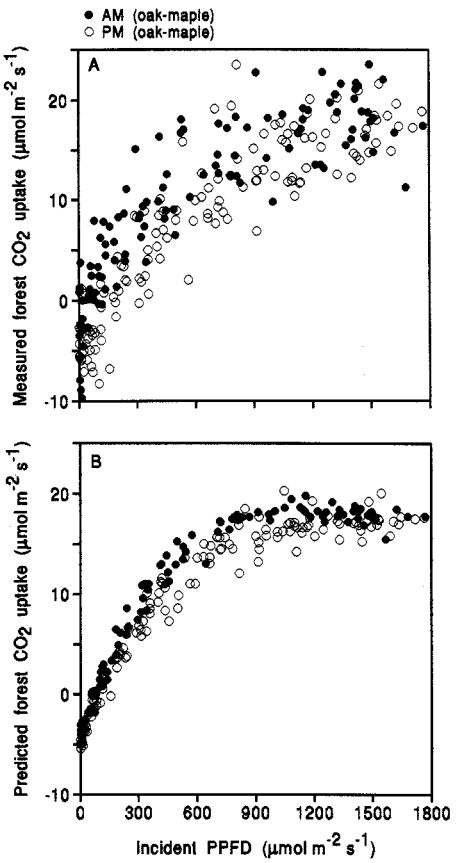

Fig. 1. (*A*) Day-time measured hourly *Quercus–Acer* forest CO_2 exchange rate as a function of mean incident PPFD during each hour when the wind was predominantly from the southwest in the period 22 July–27 September 1992. (*B*) Model predictions of day-time hourly *Quercus–Acer* forest CO_2 exchange rate as a function of incident PPFD for the same hours shown in (*A*). Closed symbols represent measurements and predictions made before noon local standard time and open symbols represent afternoon CO_2 exchange rates.

The predicted night-time hourly *Quercus–Acer* CO_2 release rate was positively correlated with the measured rate ($r \approx 0{\cdot}32$, $P < 0{\cdot}0001$). The mean predicted night-time hourly forest CO_2 release rate was *c.* 4·07 μmol CO_2 m^{-2} s^{-1}. This was significantly greater (*c.* 13%) than the mean measured rate of *c.* 3·59 μmol m^{-2} s^{-1} according to a *t*-test for paired comparisons ($P \approx 0{\cdot}007$, d.f. = 226). In any case, the *c.* 0·48 μmol CO_2 m^{-2} s^{-1} mean difference between predicted and measured night-time *Quercus–Acer* CO_2 release was small compared to whole-forest CO_2 exchange. Because the mean day-time CO_2 uptake rate predicted by the model exceeded measured rates by *c.* 1·13 μmol CO_2 m^{-2} s^{-1}, and the predicted mean night-time CO_2 release rate exceeded measured values by *c.* 0·48 μmol CO_2 m^{-2} s^{-1}, predictions of integrated daily (24 h) CO_2 uptake during the test period exceeded slightly the measured values.

Forest canopies are aerodynamically rough and relatively well ventilated. Because of this, predicted atmospheric stability and aerodynamic conductances had little effect on predicted CO_2 fluxes. That is, the explicit accounting for the physical state of the canopy airspace and buoyancy had little effect on predicted CO_2 exchange rate at the eddy correlation tower.

Short dense canopies, however, can have a much larger impact on the physical state of the canopy airspace, and the model predicts greater impacts on physiology as a result of feedbacks to the canopy airspace by such canopies (see also Jones 1992; Baldocchi 1993).

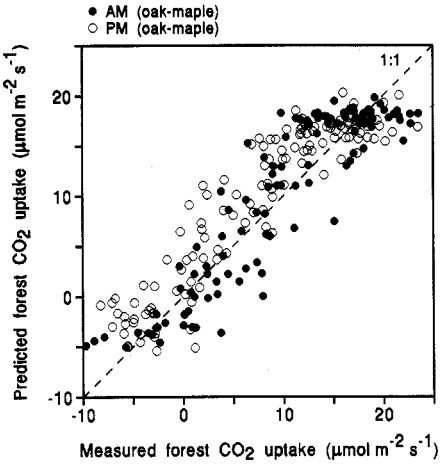

Fig. 2. Model predictions of day-time hourly *Quercus–Acer* forest CO_2 exchange versus measured day-time hourly CO_2 exchange rate during the same hours, i.e. paired comparison of CO_2 exchange rates shown in Fig. 1*A* and 1*B*.

Diel Patterns of CO_2 Exchange

Diel patterns of measured hourly average *Quercus–Acer* forest CO_2 exchange rate were in most cases accurately simulated by the model (e.g. Fig. 3). Note that Fig. 3 includes predictions of CO_2 exchange rate and eddy correlation measurements made with the hourly mean wind direction other than south-west (open symbols) and that species in addition to *Q. rubra* and *A. rubrum* might have made significant contributions to CO_2 flux in the tower footprint during those hours. In those cases too, however, predicted CO_2 exchange rate was in general agreement with measurements (we expect that *Q. rubra* and *A. rubrum* made large contributions to measured CO_2 exchange with all wind directions). Days shown in Fig. 3 were sunny, which gave rise to the strong diel patterns of CO_2 exchange rate. Diel patterns predicted for cloudy days were also consistent with measurements (not shown here; see, e.g., Fig. 5 in Amthor 1994*a*, but note that a slightly different version of the model was used to make those predictions).

Ozone Uptake

The eddy correlation measurements of O_3 uptake (mol O_3 m^{-2} ground s^{-1}) include deposition to leaf mesophyll, leaf external surfaces, tree branches and boles, and the forest floor. On the other hand, the predicted variable F_o (also mol O_3 m^{-2} ground s^{-1}) is the deposition of O_3 to the inside of leaves only. Nonetheless, we view the comparison between predicted and measured O_3 uptake as a test of predicted canopy and leaf surface gas conductances. Measured whole-forest O_3 uptake rate should equal or exceed F_o, unless the forest is a source of O_3.

Predicted and measured day-time rates of O_3 uptake were positively correlated ($r \approx +0{\cdot}76$, $P < 0{\cdot}0001$) during the 227 day-time test hours when the wind was from the south-west and when O_3 uptake was measured. Maximum measured whole-forest O_3 uptake rate was *c.* 20 nmol m^{-2} s^{-1} whereas maximum predicted F_o was *c.* 15 nmol m^{-2} s^{-1}. The mean predicted day-time hourly rate of O_3 uptake into *Quercus–Acer* leaves (*c.* 5·75 nmol m^{-2} s^{-1}) was *c.* 10% smaller than the mean measured hourly O_3 uptake rate by the whole forest (6·42 nmol m^{-2} s^{-1}); according to a *t*-test for paired comparisons, the two means were different ($P \approx 0{\cdot}0008$, d.f. = 226).

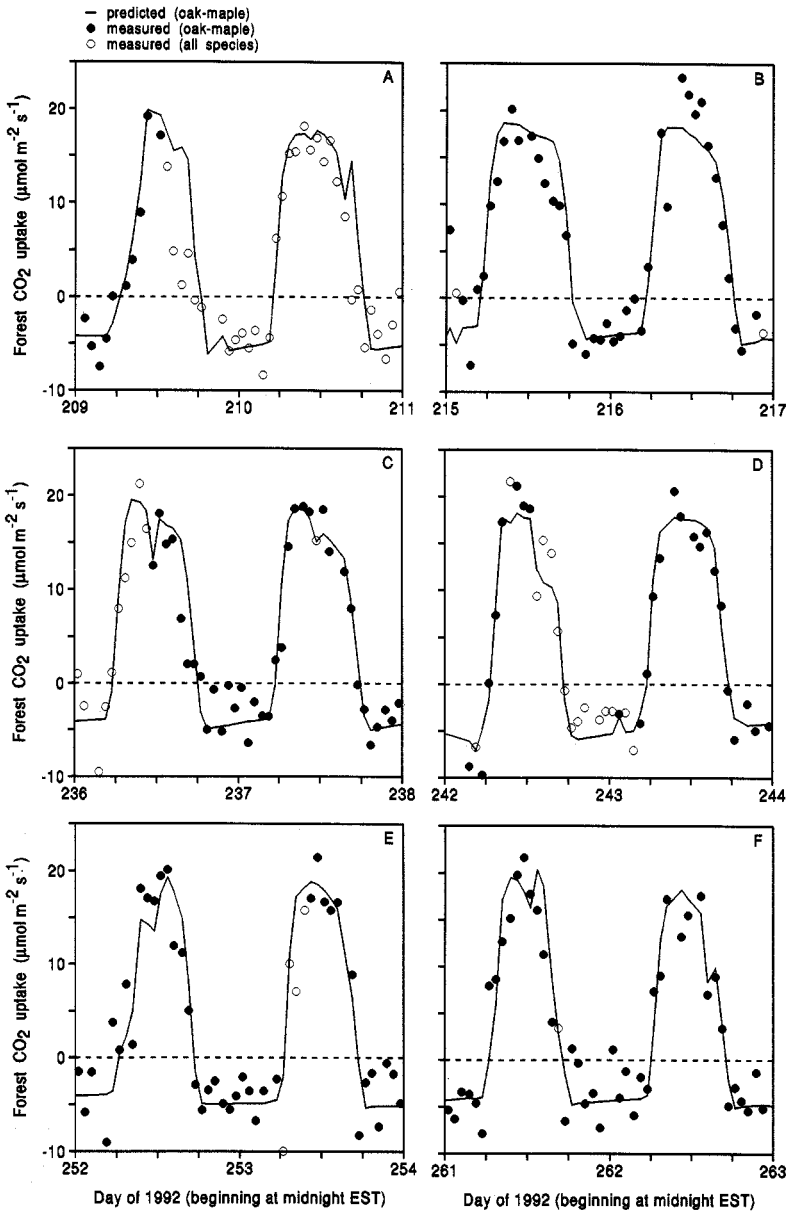

Fig. 3. Diel course of predicted and measured *Quercus–Acer* forest CO_2 exchange (lines and closed symbols, respectively) during six 48 h intervals (panels *A–F*, respectively) with nearly complete eddy correlation data during the 68 day model test period. Eddy correlation measurements made when the wind was not predominantly from the southwest, i.e. when species in addition to *Quercus* and *Acer* may have also contributed significantly to measured CO_2 exchange, are shown for comparison (open symbols). PPFD was relatively high during most of the midday hours of these 12 days.

Analysis of O_3 flux data at night and in winter at this site indicates that O_3 deposition to non-foliar surfaces accounts for up to 25% of whole-forest O_3 uptake at midday (J. W. Munger *et al.*, unpublished data). Morning and midday values of F_o were broadly consistent with these site estimates of O_3 deposition to non-leaf surfaces (Fig. 4). Moreover, measured O_3 uptake nearly always exceeded predicted uptake into leaves at night when stomata were presumably closed. As evident for several days, however, the model overpredicted O_3 uptake during the afternoon (e.g. Fig. 4). In this respect, the predicted rate of O_3 uptake was more tightly coupled to O_a during the day, compared to the measured uptake rate. For example, daily maximum O_a occurred at about 2030 hours on day 215 (at a level of 7 mPa) and 1700 hours on day 216 (at a level greater than 9 mPa) and the model predicted relatively rapid afternoon O_3 uptake compared to measurements during the afternoon of days 215 and 216 (Fig. 4*B*). This indicates that afternoon stomatal conductance was overpredicted, which may explain the overprediction of afternoon CO_2 uptake (Fig. 2).

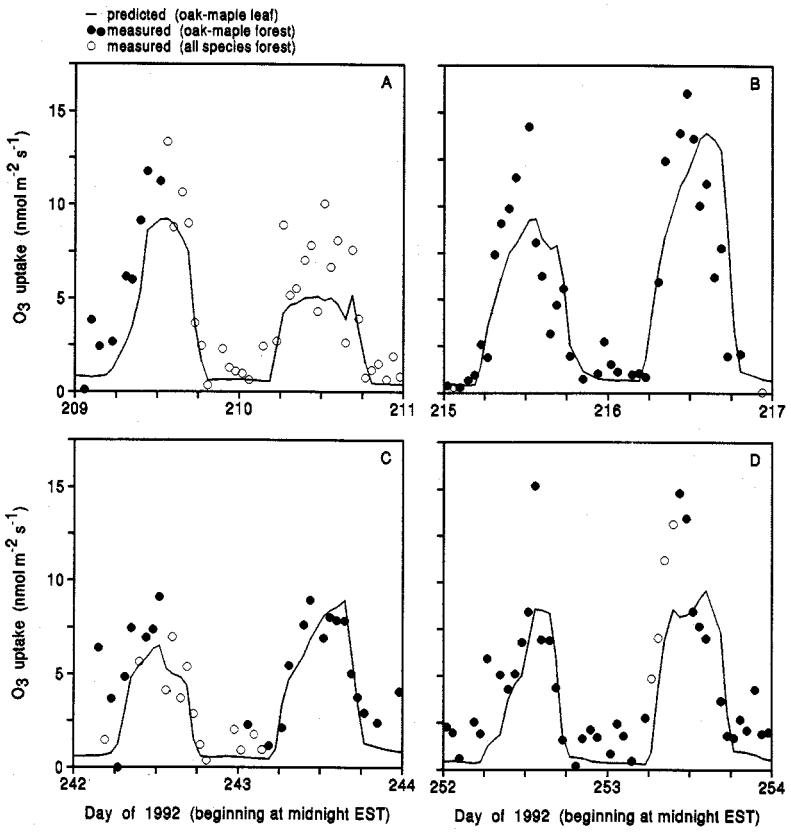

Fig. 4. Same as Fig. 3 but, instead of CO_2 exchange, predicted and measured O_3 uptake is shown, and only four sets of 48 h periods are given. Predicted O_3 uptake is into leaves only, whereas measured uptake is total deposition to the forest.

Ozone may be phytotoxic at levels of 5–10 mPa, and high afternoon O_a, e.g. 9 mPa on day 216 and greater than 11 mPa on day 237, may have inhibited photosynthesis to a significant degree at the eddy correlation site. The day-time values of α_{ozone} predicted by the model implied that O_3 at the eddy correlation site might have inhibited photosynthesis *c.* 5–15% on many days. While we have no independent measure of effects of ambient O_3

on photosynthesis at the eddy correlation site, we note that there is evidence that ambient air pollution in the north-eastern US may limit growth of trees in the field (e.g. Wang *et al.* 1986). Afternoon CO_2 uptake may also be limited following morning and midday O_3 uptake due to enhanced leaf maintenance respiration (e.g. Amthor and Cumming 1988). This possibility was not addressed by the present model because it does not include a respiratory response to O_3 uptake.

CO_2 Partial Pressures and Gradients

Diel minima of C_a typically occurred near midday or during the afternoon in the test period. Minimum daily values of C_a during sunny days was regularly in the range 33–34 Pa. C_a maxima typically occurred at about sunrise, with values commonly in the range 35–38 Pa.

The model predicts CO_2 partial pressures (in Pa) in the canopy airspace C_{can}, the leaf intercellular spaces C_i, and the chloroplast stroma C_c. During the day-time, C_{can} was slightly lower than C_a. This had only a minor impact on canopy photosynthesis. The day-time ratio of C_i to C_{can} was generally in the range 0·65–0·70 because of the chosen value of k_{stoma}. That is, k_{stoma} was set so that this ratio would be obtained under 'normal' conditions at the test site. The value of C_i is important to g_s (the two are negatively related) and P_s (the two are positively related).

The model predicted that the ratio of C_c to C_{can} was typically in the range 0·50–0·60 during sunny days. A value of 0·54 for *Q. rubra* C_c/C_{can} has been estimated in laboratory experiments with leaves with a high boundary layer conductance (Loreto *et al.* 1992). The value of C_c is directly linked to P_s in the model because it is C_c (albeit in combination with other factors) that determines CO_2 assimilation rate and the ratio of RuP_2 carboxylation to oxygenation, i.e. the ratio of photosynthesis to photorespiration. As expected, values of C_a, C_{can}, C_i, and C_c were generally higher on cloudy days than on sunny days.

At night, measured and predicted C_{can} generally exceeded C_a by one to several Pa, depending on wind speed and temperature, whereas the predicted night-time ratio of C_i to C_{can} was generally in the range 1·1–1·3, depending mostly on temperature through its effect on leaf respiration rate (R_d, mol CO_2 m^{-2} s^{-1}).

The model predicts a slight decline in the ratio of C_i to C_{can} with an increase in photosynthesis brought about by an increase in $f_{rub}N$ (not shown). This response has been measured for individual leaves of the C_3 species *Gossypium hirsutum* by Wong *et al.* (1985), but we do not know if a similar relationship exists between canopy photosynthesis and canopy C_i in nature.

This big-leaf model is based on f_{rub} and N rather than a specified CO_2 exchange rate because their product is linked fundamentally to the RuP_2-saturated rate of carboxylation and it makes a direct connection between plant nitrogen and carbon cycles. A different approach is to estimate photosynthetic capacity by empirical observation at a site, but such observations may be affected by stress, measurement error, or variation in leaf nitrogen content. Measurements of leaf CO_2 exchange rate are also more difficult than measurements of leaf nitrogen content. The challenge for use of the present model is evaluating f_{rub}. Indeed, this approach has traded the difficulties of estimating photosynthetic capacity by using leaf CO_2 exchange measurements for the difficulties of obtaining estimates of f_{rub}. One hope is that f_{rub} may be related to plant or ecosystem 'functional type' or some other coarse categorisation scheme and that N can be evaluated remotely, say from satellite observations, so that the model could be applied to large areas without the need for a network of ground-based leaf CO_2 exchange measurements.

Apparent Afternoon Limitation on Photosynthesis and Stomatal Conductance

The maximum rate of measured CO_2 uptake by the forest on a given day generally occurred before noon. In particular, the afternoon rate of CO_2 uptake was often lower

than the rate in the morning at the same PPFD for a given date (compare filled and open symbols in Fig. 1*A*). This same result was reported by Wofsy *et al.* (1993) for the 1990 and 1991 measurements at the eddy correlation site. Greater morning compared to afternoon ecosystem CO_2 uptake has been observed in other forests as well (e.g. Fan *et al.* 1990; Hollinger *et al.* 1994).

We cannot, at present, resolve completely the reasons for the measured midmorning maxima in CO_2 assimilation at the eddy correlation site. The model predicted some morning maxima in CO_2 uptake followed by afternoon declines at a given PPFD (compare filled and open symbols in Fig. 1*B* and see solid lines in Fig. 3*A*–F). These predictions were the result of a combination of stomatal response to increased vapour pressure difference between the inside and the outside of the big leaf in the afternoon when temperature was high compared to the morning, and to increased O_3 uptake and inhibition of photosynthesis due to increased O_a in the afternoon compared to morning. Conversely, the small decline in C_a in the late afternoon had little effect on forest CO_2 assimilation according to the model, which accounts for effects of C_a on CO_2 assimilation by mechanistic means. Marked midmorning maxima in individual leaf surface conductances have been observed in hardwoods followed by midday and afternoon declines (e.g. Kozlowski *et al.* 1991), patterns that are consistent with the predicted and measured reductions in afternoon CO_2 uptake at the eddy correlation site. The model did not, however, predict the exact pattern of diurnal CO_2 uptake by the forest; on average, predicted CO_2 uptake exceeded measured *Quercus–Acer* CO_2 uptake during the late afternoon on the test dates (Fig. 5). This indicates a stronger afternoon response to Δe or O_3 by the actual forest compared to the model, or the existence of additional factors limiting photosynthesis in the forest in the afternoon, or both.

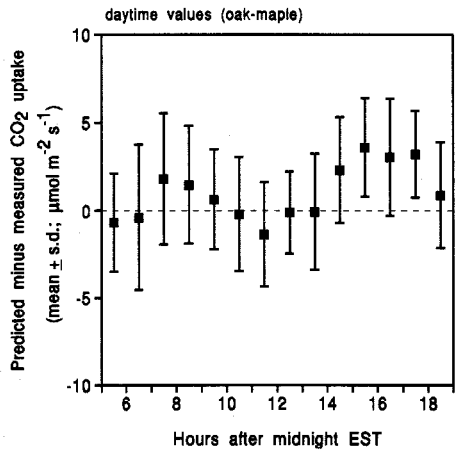

Fig. 5. Mean difference (± standard deviation) between predicted and measured day-time hourly *Quercus–Acer* forest CO_2 uptake as a function of time of the day during the 68 day test period. All predictions and measurements are centred on the half-hour (local standard time). The number of observations during each hour ranged from 11 to 22.

One possible additional factor is that equations for R_{soil} and R_{stem}, which were based on T_s and derived from only night-time CO_2 exchange measurements, may have underestimated day-time R_{forest}, especially in the afternoon, the warmest part of the day with respect to T_a.

The overprediction of afternoon g_s that is apparent in the comparison of predicted and measured O_3 uptake (Fig. 4), however, indicated that an underestimation of R_{soil} or R_{stem} could not account fully for the overprediction of afternoon CO_2 uptake, but rather that P_s was too fast as a result of exaggerated CO_2 supply to chloroplasts. On the whole, predictions of O_3 uptake compared to measurements of uptake imply that predicted conductances of water vapour and CO_2 from the reference height z to the intercellular spaces were relatively accurate early in the day, but were too high in the afternoon.

Feedback inhibition of photosynthesis by carbohydrate accumulation in leaves, perhaps because source activity exceeded sink activity (Herold 1980), may have slowed afternoon CO_2 uptake and reduced g_s (Azcón-Bieto 1983). One reason to combine this canopy physiology model with a whole-plant growth and respiration model, therefore, is to account for feedbacks between source and sink activity. Our results imply that such feedbacks may be important to predictions of canopy physiology during afternoon periods.

Conclusions

The big-leaf canopy model is elementary and involves many simplifications of the present state of knowledge. Nonetheless, it accounts for the aspects of canopy physiology known to be important to mass and energy exchange with the atmosphere. Model predictions of CO_2 exchange were in excellent agreement with measured CO_2 exchange on both hourly and daily temporal scales. Based on this success, we conclude that the forest responds primarily to the environmental parameters PPFD, temperature, and vapour pressure. (Soil moisture was high during the test period, but the model predicts that low soil moisture would significantly effect CO_2 exchange, as has been commonly observed.) Furthermore, spatial heterogeneity in the forest did not cause large differences between measured and predicted CO_2 fluxes; the big-leaf model predictions of CO_2 exchange were not significantly compromised by treating the canopy as a single homogeneous collection of leaves.

The model underpredicted forest O_3 uptake in the morning and at midday, but that was expected because the model does not account for O_3 deposition to leaf external surfaces, stems, or the soil. Indeed, the difference between predicted O_3 uptake into leaves and the measured rates of O_3 deposition to the whole forest in the morning and at midday are consistent with independent estimates of deposition to non-leaf surfaces. A comparison of predicted and measured afternoon uptake of O_3, however, suggested that predicted conductance exceeded actual conductance during afternoon periods. This was also reflected in afternoon overpredictions of forest CO_2 uptake. These results suggest that model refinements should account for source–sink interactions and perhaps include a detailed treatment of whole-tree water relations. Respiratory responses to O_3 and long-term effects of O_3 on photosynthesis might also be added to the model.

We reiterate that this work represents an *independent* test of the model. Model development and testing proceeded in the following order: (1) the big-leaf model was developed independently of the eddy correlation measurements; (2) the model was parameterised for a *Quercus–Acer* stand near the eddy correlation tower without reference to any day-time CO_2 exchange measurements made at or near the site; (3) the model was solved using environmental parameters measured at the eddy correlation tower during a 68 day period in summer and early autumn of 1992; and then (4) the model predictions were compared to the measurements of whole-forest CO_2 and O_3 exchange made by the eddy correlation method. We appreciate that there are limitations imposed by a big-leaf model (see, e.g., Field 1991), but believe that a big-leaf canopy physiology model is a practical solution to the need for large-scale ecosystem level predictions of mass and energy exchange. This is particularly the case with respect to assessing impacts of global increases in atmospheric CO_2 and other environmental changes. Moreover, this test of the model suggests that it is fundamentally sound and that the forest canopy did behave in many respects as a rather simple big leaf. Improvements to the model can be made, and some are now underway, but the basic model structure and equations are suitable for many applications. Nonetheless, the big-leaf canopy physiology model must be combined with models of tree growth, non-leaf respiration, root turnover, litterfall, and litter and soil organic matter decomposition to predict the full carbon cycle of a forest. The eddy correlation method is an important tool for testing and improving canopy and whole-forest physiology and carbon cycle models as demonstrated in this study.

Acknowledgments

Eddy correlation measurements at Harvard Forest were supported by grants to Harvard University from the US National Science Foundation (BSR-8919300), the US National Aeronautics and Space Administration (NAGW-3082), the US Department of Energy's (DOE) National Institute for Global Environmental Change (NIGEC) through the NIGEC Northeast Regional Center at Harvard University (DOE Cooperative Agreement No. DE-FC03-90ER61010), and Harvard University (Harvard Forest and Division of Applied Science). Modelling was supported by grants from the NIGEC Northeast Regional Center and the Andrew W. Mellon Foundation to the Woods Hole Research Center and by the Lawrance Livermore National Laboratory's (LLNL) Laboratory Directed Research and Development Program. Work at LLNL was performed under the auspices of the US DOE under Contract No. W-7405-Eng-48. Two anonymous reviewers made useful comments.

References

Aber, J. D., Magill, A., Boone, R., Melillo, J. M., Steudler, P., and Bowden, R. (1993). Plant and soil responses to chronic nitrogen addition at the Harvard Forest, Massachusetts. *Ecological Applications* **3**, 156–166.

Amthor, J. S. (1994*a*). Scaling CO_2-photosynthesis relationships from the leaf to the canopy. *Photosynthesis Research* **39**, 321–350.

Amthor, J. S. (1994*b*). Respiration and carbon assimilate use. In 'Physiology and Determination of Crop Yield'. (Eds K. J. Boote, J. M. Bennett, T. R. Sinclair and G. M. Paulsen.) pp. 221–250. (American Society of Agronomy: Madison, Wisconsin.)

Amthor, J. S., and Cumming, J. R. (1988). Low levels of ozone increase bean leaf maintenance respiration. *Canadian Journal of Botany* **66**, 724–726.

Aphalo, P. J., and Jarvis, P. G. (1993). The boundary layer and the apparent responses of stomatal conductance to wind speed and to the mole fractions of CO_2 and water vapour in the air. *Plant, Cell and Environment* **16**, 771–783.

Azcón-Bieto, J. (1983). Inhibition of photosynthesis by carbohydrates in wheat leaves. *Plant Physiology* **73**, 681–686.

Baldocchi, D. D. (1993). Scaling water vapor and carbon dioxide exchange from leaves to a canopy: rules and tools. In 'Scaling Physiological Processes: Leaf to Globe'. (Eds J. R. Ehleringer and C. B. Field.) pp. 77–114. (Academic Press: San Diego.)

Baldocchi, D. D., Hutchison, B. A., Matt, D. R., and McMillen, R. T. (1985). Canopy radiative transfer models for spherical and known leaf inclination angle distributions: a test in an oak-hickory forest. *Journal of Applied Ecology* **22**, 539–555.

Baldocchi, D. D., Verma, S. B., and Anderson, D. E. (1987). Canopy photosynthesis and water-use efficiency in a deciduous forest. *Journal of Applied Ecology* **24**, 251–260.

Baldocchi, D. D., Hicks, B. B., and Meyers, T. P. (1988). Measuring biosphere–atmosphere exchanges of biologically related gases with micrometeorological methods. *Ecology* **69**, 1331–1340.

Bolin, B., Degens, E. T., Duvigneaud, P., and Kempe, S. (1979). The global biogeochemical carbon cycle. In 'The Global Carbon Cycle'. (Eds B. Bolin, E. T. Degens, S. Kempe and P. Ketner) pp. 1–56. (Wiley: Chichester.)

Brent, R. P. (1973). 'Algorithms for Minimization Without Derivatives.' (Prentice-Hall: Englewood Cliffs, New Jersey.)

Brutsaert, W. (1982). 'Evaporation into the Atmosphere.' (D. Reidel: Dordrecht.)

Bussinger, J. A. (1975). Aerodynamics of vegetated surfaces. In 'Heat and Mass Transfer in the Biosphere. I. Transfer Processes in the Plant Environment'. (Eds D. A. de Vries and N. H. Afgan.) pp. 139–165. (Wiley: New York.)

Caldwell, M. M., Meister, H.-P., Tenhunen, J. D., and Lange, O. L. (1986). Canopy structure, light microclimate and leaf gas exchange of *Quercus coccifera* L. in a Portuguese macchia: measurements in different canopy layers and simulations with a canopy model. *Trees* **1**, 25–41.

Caldwell, M. M., Matson, P. A., Wessman, C., and Gamon, J. (1993). Prospects for scaling. In 'Scaling Physiological Processes: Leaf to Globe'. (Eds J. R. Ehleringer and C. B. Field.) pp. 223–230. (Academic Press: San Diego.)

Choudhury, B. J., and Monteith, J. L. (1988). A four-layer model for the heat budget of homogeneous land surfaces. *Quarterly Journal of the Royal Meteorological Society* **114**, 373–398.

Collatz, G. J., Ball, J. T., Grivet, C., and Berry, J. A. (1991). Physiological and environmental regulation of stomatal conductance, photosynthesis and transpiration: a model that includes a laminar boundary layer. *Agricultural and Forest Meteorology* **54**, 107–136.

Dabberdt, W. F., Lenschow, D. H., Horst, T. W., Zimmerman, P. R., Oncley, S. P., and Delany, A. C. (1993). Atmosphere–surface exchange measurements. *Science* **260**, 1472–1481.

Ellsworth, D. S., and Reich, P. B. (1993). Canopy structure and vertical patterns of photosynthesis and related leaf traits in a deciduous forest. *Oecologia* **96**, 169–178.

Eltahir, E. A. B., and Bras, R. L. (1993). On the response of the tropical atmosphere to large-scale deforestation. *Quarterly Journal of the Royal Meteorological Society* **119**, 779–793.

Erbs, D. G., Klein, S. A., and Duffie, J. A. (1982). Estimation of the diffuse radiation fraction for hourly, daily and monthly-average global radiation. *Solar Energy* **28**, 293–302.

Evans, J. R. (1989). Photosynthesis and nitrogen relationships in leaves of C_3 plants. *Oecologia* **78**, 9–19.

Fan, S.-M. Wofsy, S. C., Bakwin, P. S., Jacob, D. J., and Fitzjarrald, D. R. (1990). Atmosphere–biosphere exchange of CO_2 and O_3 in the central Amazon forest. *Journal of Geophysical Research* **95**, 16851–16864.

Farquhar, G. D. (1989). Models of integrated photosynthesis of cells and leaves. *Philosophical Transactions of the Royal Society of London* B **323**, 357–367.

Farquhar, G. D., and Wong, S. C. (1984). An empirical model of stomatal conductance. *Australian Journal of Plant Physiology* **11**, 191–210.

Farquhar, G. D., Caemmerer, S. von, and Berry, J. A. (1980). A biochemical model of photosynthetic CO_2 assimilation in leaves of C_3 species. *Planta* **149**, 78–90.

Field, C. B. (1991). Ecological scaling of carbon gain to stress and resource availability. In 'Response of Plants to Multiple Stresses'. (Eds H. A. Mooney, W. E. Winner and E. J. Pell.) pp. 35–65. (Academic Press: San Diego.)

Fitzjarrald, D. R., and Moore, K. E. (1990). Mechanisms of nocturnal exchange between the Amazon forest and the atmosphere. *Journal of Geophysical Research* **95**, 16839–16850.

Friend, A. D. (1991). Use of a model of photosynthesis and leaf microenvironment to predict optimal stomatal conductance and leaf nitrogen partitioning. *Plant, Cell and Environment* **14**, 895–905.

Gollan, T., Passioura, J. B., and Munns, R. (1986). Soil water status affects the stomatal conductance of fully turgid wheat and sunflower leaves. *Australian Journal of Plant Physiology* **13**, 459–464.

Grace, J. (1991). Physical and ecological evaluation of heterogeneity. *Functional Ecology* **5**, 192–201.

Grantz, D. A. (1990). Plant response to atmospheric humidity. *Plant, Cell and Environment* **13**, 667–679.

Herold, A. (1980). Regulation of photosynthesis by sink activity—the missing link. *New Phytologist* **86**, 131–144.

Hollinger, D. Y., Kelliher, F. M., Byers, J. N., Hunt, J. E., McSeveny, T. M., and Weir, P. L. (1994). Carbon dioxide exchange between an undisturbed old-growth temperate forest and the atmosphere. *Ecology* **75**, 134–150.

Jones, H. G. (1992). 'Plants and Microclimate.' 2nd edn. (Cambridge University Press: Cambridge.)

Kirschbaum, M. U. F., and Farquhar, G. D. (1984). Temperature dependence of whole-leaf photosynthesis in *Eucalyptus pauciflora* Sieb. ex Spreng. *Australian Journal of Plant Physiology* **11**, 519–538.

Kozlowski, T. T., Kramer, P. J., and Pallardy, S. G. (1991). 'The Physiological Ecology of Woody Plants.' (Academic Press: San Diego.)

Laisk, A., Kull, O., and Moldau, H. (1989). Ozone concentration in leaf intercellular air spaces is close to zero. *Plant Physiology* **90**, 1163–1167.

Lauer, M. L., and Boyer, J. S. (1992). Internal CO_2 measured directly in leaves. *Plant Physiology* **98**, 1310–1316.

Lee, J., and Bowling, D. J. F. (1992). Effect of the mesophyll on stomatal opening in *Commelina communis*. *Journal of Experimental Botany* **43**, 951–957.

Leuning, R., and King, K. M. (1992). Comparison of eddy-covariance measurements of CO_2 fluxes by open- and closed-path CO_2 analyzers. *Boundary Layer Meteorology* **59**, 297–311.

Loomis, R. S., Rabbinge, R., and Ng, E. (1979). Explanatory models in crop physiology. *Annual Review of Plant Physiology* **30**, 339–367.

Loreto, F., Harley, P. C., Di Marco, G., and Sharkey, T. D. (1992). Estimation of mesophyll conductance to CO_2 flux by three different methods. *Plant Physiology* **98**, 1437–1443.

Makino, A., and Osmond, B. (1991). Effects of nitrogen nutrition on nitrogen partitioning between chloroplasts and mitochondira in pea and wheat. *Plant Physiology* **96**, 355–362.

McMillen, R. T. (1988). An eddy correlation technique with extended applicability to non-simple terrain. *Boundary Layer Meteorology* **43**, 231–245.

Michalsky, J. J. (1988). *The Astronomical Almanac's* algorithm for approximate solar position (1950–2050). *Solar Energy* **40**, 227–235.

Monteith, J. L. (1973). 'Principles of Environmental Physics.' (Edward Arnold: London.)

Mott, K. A. (1988). Do stomata respond to CO_2 concentrations other than intercellular? *Plant Physiology* **86**, 200–203.

Mott, K. A., and Parkhurst, D. F. (1991). Stomatal responses to humidity in air and helox. *Plant, Cell and Environment* **14**, 509–515.

Norman, J. M. (1980). Interfacing leaf and canopy light interception models. In 'Predicting Photosynthesis for Ecosystem Models'. Vol. II. (Eds J. D. Hesketh and J. W. Jones.) pp. 49–67. (CRC Press: Boca Raton, Florida.)

Norman J. M. (1989). Synthesis of canopy processes. In 'Plant Canopies: Their Growth, Form and Function'. (Eds G. Russell, B. Marshall and P. G. Jarvis.) pp. 161–175. (Cambridge University Press: Cambridge.)

Norman J. M. (1993). Scaling processes between leaf and canopy levels. In 'Scaling Physiological Processes: Leaf to Globe'. (Eds J. R. Ehleringer and C. B. Field.) pp. 41–76. (Academic Press: San Diego.)

Norman, J. M., and Polley, W. (1989). Canopy photosynthesis. In 'Photosynthesis'. (Ed. W. R. Briggs.) pp. 227–241. (Alan R. Liss: New York.)

Penning de Vries, F. W. T. (1983). Modeling of growth and production In 'Physiological Plant Ecology IV'. (Eds O. L. Lange, P. S. Nobel, C. B. Osmond, and H. Ziegler.) Encyclopedia of Plant Physiology, New Series, Vol. 12D, pp. 117–150. (Springer-Verlag: Berlin.)

Reich, P. B., and Amundson, R. G. (1985). Ambient levels of ozone reduce net photosynthesis in tree and crop species. *Science* **230**, 566–570.

Ryan, M. G. (1991). Effects of climate change on plant respiration. *Ecological Applications* **1**, 157–167.

Sadras, V. O., Hall, A. J., and Connor, D. J. (1993). Light-associated nitrogen distribution profile in flowering canopies of sunflower (*Helianthus annuus* L.) altered during grain growth. *Oecologia* **95**, 488–494.

Sellers, P. J., Berry, J. A., Collatz, G. J., Field, C. B., and Hall, F. G. (1992). Canopy reflectance, photosynthesis, and transpiration. III. A reanalysis using improved leaf models and a new canopy integration scheme. *Remote Sensing of Environment* **42**, 187–216.

Shukla, J., Nobre, C., and Sellers, P. (1990). Amazon deforestation and climate change. *Science* **247**, 1322–1325.

Shuttleworth, W. J., and Wallace, J. S. (1985). Evaporation from sparse crops—an energy combination theory. *Quarterly Journal of the Royal Meteorological Society* **111**, 839–855.

Sinclair, T. R., Murphy, C. E., Jr, and Knoerr, K. R. (1976). Development and evaluation of simplified models for simulating canopy photosynthesis and transpiration. *Journal of Applied Ecology* **13**, 813–829.

Sokal, R. R., and Rohlf, F. J. (1981). 'Biometry.' 2nd edn. (Freeman: New York.)

Swinbank, W. C. (1951). The measurement of vertical transfer of heat and water vapor by eddies in the lower atmosphere. *Journal of Meteorology* **8**, 135–145.

Szeicz, G. (1974). Solar radiation for plant growth. *Journal of Applied Ecology* **11**, 617–636.

Tardieu, F., and Davies, W. J. (1993). Integration of hydraulic and chemical signalling in the control of stomatal conductance and water status of droughted plants. *Plant, Cell and Environment* **16**, 341–349.

Thom, A. S. (1968). The exchange of momentum, mass, and heat between an artificial leaf and the airflow in a wind-tunnel. *Quarterly Journal of the Royal Meteorological Society* **94**, 44–55.

Wang, D., Bormann, F. H., and Karnosky, D. F. (1986). Regional tree growth reductions due to ambient ozone: evidence from field experiments. *Environmental Science & Technology* **20**, 1122–1125.

Wang, Y.-P., McMurtrie, R. E., and Landsberg, J. J. (1992). Modelling canopy photosynthetic productivity. In 'Crop Photosynthesis: Spatial and Temporal Determinants'. (Eds N. R. Baker and H. Thomas.) pp. 43–67. (Elsevier Science Publishers: Amsterdam.)

Waring, R. H., and Schlesinger, W. H. (1985). 'Forest Ecosystems: Concepts and Management.' (Academic Press: Orlando.)

Wofsy, S. C., Goulden, M. L., Munger, J. W., Fan, S.-M., Bakwin, P. S., Daube, B. C., Bassow, S. L., and Bazzaz, F. A. (1993). Net exchange of CO_2 in a mid-latitude forest. *Science* **260**, 1314–1317.

Wong, S.-C., Cowan, I. R., and Farquhar, G. D. (1985). Leaf conductance in relation to rate of CO_2 assimilation. I. Influence of nitrogen nutrition, phosphorus nutrition, photon flux density, and ambient partial pressure of CO_2 during ontogeny. *Plant Physiology* **78**, 821–825.

Woodrow, I. E., and Berry, J. A. (1988). Enzymatic regulation of photosynthetic CO_2 fixation in C_3 plants. *Annual Review of Plant Physiology and Plant Molecular Biology* **39**, 533–594.

Wullschleger, S. D. (1993). Biochemical limitations to carbon assimilation in C_3 plants–a retrospective analysis of the A/C_i curves from 109 species. *Journal of Experimental Botany* **44**, 907–920.

Appendix
A Big-leaf Model of Steady-state Canopy Mass and Energy Exchange

This one-dimensional steady-state big-leaf canopy model combines leaf and canopy mass and energy transport equations with a model of leaf mesophyll carbon metabolism using parameters defined in Tables 1 (input variables) and 2 (calculated variables). The model is solved by calculating all variables that remain constant for a given set of environmental conditions, picking 'starting values' for T_c, u_*, e_c, C_{can}, g_s, T_ℓ and C_c, and iteratively solving the full model until a steady state is reached (Table 3). All area-based parameters (i.e. parameters with unit m^{-2}) except g_c and $g_{s(min)}$ are on a ground area basis.

Energy, Water and Momentum Exchange

The canopy airspace is bounded on the bottom by the forest floor and extends upwards to the top of the canopy at height h. (In nature, forest h is not constant but varies horizontally; in the model, however, it is uniform.) Inclusion of an explicit canopy airspace that can differ from the atmosphere at the reference height z allows the model to account for feedbacks from the plants and soil to the canopy airspace which in turn affects canopy physiology. Air temperature, water vapour pressure, and CO_2 partial pressure are assumed to be uniform (homogeneous) throughout the canopy airspace, which is an obvious simplification of nature.

Atmospheric Stability and Conductances

Zero plane displacement height d and roughness length z_M are calculated according to Choudhury and Monteith (1988), and z_H is then defined, as follows

$$d = 1{\cdot}1\, h \ln [1 + (c_d L)^{\frac{1}{4}}] \tag{A1}$$

$$z_M = z_S + 0{\cdot}3\, h\, (c_d L)^{\frac{1}{2}} \qquad \text{for } (c_d L) \leq 0{\cdot}2 \tag{A2a}$$

$$z_M = 0{\cdot}3\,h\,(1 - d/h) \qquad \text{for } (c_d L) > 0{\cdot}2 \tag{A2b}$$

$$z_H = 0{\cdot}2\,z_M\,, \tag{A3}$$

where ln (x) denotes $\log_e x$.

Atmospheric stability ζ, stability correction parameter for momentum Ψ_M, stability correction parameter for heat Ψ_H, friction velocity u_*, atmospheric conductances (i.e. from outside the leaf boundary layer to the reference height z), and momentum flux density τ are calculated in an iterative manner from the following relationships (after Brutsaert 1982)

$$E = g_{aW}\,[e_c - e_a]/P \tag{A4}$$

$$H = c_p\,\rho\,g_{aH}\,(T_c - T_a) \tag{A5}$$

$$\zeta = -\kappa g z\,(H/[c_p\,(273{\cdot}15 + T_a)] + 0{\cdot}01099E)/(\rho\,u_*^3) \tag{A6}$$

$$x = (1 - 16\,\max\{-1,\ \zeta\})^{\frac{1}{4}} \qquad \text{for } \zeta \leq 0 \tag{A7a.1}$$

$$\Psi_H = 2\ln[(1 + x^2)/2] \qquad \text{for } \zeta \leq 0 \tag{A7a.2}$$

$$\Psi_M = 2\ln[(1 + x)/2] + \Psi_H/2 - 2\tan^{-1}(x) + \pi/2 \qquad \text{for } \zeta \leq 0 \tag{A7a.3}$$

$$\Psi_M = \Psi_H = -5{\cdot}2\,\min\{1, \zeta\} \qquad \text{for } \zeta > 0 \tag{A7b}$$

$$u_* = \kappa u(z)/(\ln[(z - d)/z_M] - \Psi_M) \tag{A8}$$

$$g_{aH} = \kappa u_*/(\ln[(z - d)/z_H] - \Psi_H) \tag{A9}$$

$$g_{aW} = g_{aH} P/[R\,(273{\cdot}15 + T_a)] \tag{A10}$$

$$\tau = \rho u_*^2\,, \tag{A11}$$

where g is gravitational acceleration ($9{\cdot}8\ \mathrm{m\ s^{-2}}$), x is an intermediate variable, max $\{a, b\}$ denotes maximum of a and b, and min $\{a, b\}$ denotes minimum of a and b. Atmospheric stability ζ is the reference height z divided by Obukhov's stability length including the effect of water vapour flux E (Brutsaert 1982, his equation [4·25]). The max $\{-1, \zeta\}$ and min $\{1, \zeta\}$ functions limit effects of extremes in ζ on Ψ_H and Ψ_M.

Wind speed outside the leaf boundary layer but inside the canopy ($u(c)$, $\mathrm{m\ s^{-1}}$) and leaf boundary layer conductances g_b and g_{bH} are then approximated by (references in Amthor 1994*a*)

$$u(c) = (u_*/\kappa)\,\ln[(h - d)/z_M]\,\exp[\alpha_{wind}(d/h - 1)] \tag{A12}$$

$$\delta = 0{\cdot}004\,[\ell/u(c)]^{\frac{1}{2}}/L \tag{A13}$$

$$g_{bH} = 2\,D_H/\delta \tag{A14}$$

$$g_b = P\,D_{wv}(1 + s_r)^2/[\delta(1 + s_r^2)R(273{\cdot}15 + T_a)]\,, \tag{A15}$$

where D_H is the diffusion coefficient of heat in air, which is a $f(T_a)$, and 2 in equation (A14) accounts for heat exchange with both top and bottom leaf surfaces.

Radiation Balance

Solar radiation balance of the canopy (model components 1 and 2) is described in Amthor (1994*a*). For this model test, leaf and soil optical properties were taken from Baldocchi *et al.* (1985) who studied a *Quercus–Carya* forest in Tennessee, USA. The parameter c is a leaf clumping term. Total shortwave radiation absorption I_a is the sum of absorbed NIR and PAR.

Longwave radiation absorption and emission by the canopy are approximated by

$$L_a = \alpha_\ell[1 - \exp(-c\,L)][L_{down} + L_{soil}] \tag{A16}$$

$$L_e = 2\,\alpha_\ell[1 - \exp(-c\,L)]\sigma(273{\cdot}15 + T_a)^4, \tag{A17}$$

where $[1-\exp(-c\,L)]$ is the fraction of incident diffuse radiation that strikes a leaf in the canopy and 2 in equation (A17) accounts for emission from both leaf surfaces.

Canopy Sensible and Latent Heat Exchange and Temperature

Steady-state canopy transpiration rate E_ℓ, sensible heat exchange H_ℓ, and temperature T_ℓ are given by

$$\Delta e = e_\ell - e_c + E_\ell P/g_b \qquad \Delta e \geq 0 \tag{A18}$$

$$g_s = \xi[g_{s(min)}L + k_{stoma}\exp(-0{\cdot}00045\,\Delta e)P_s/C_i] \tag{A19}$$

$$g_w = 1/[1/(g_c L + g_s) + 1/g_b] \qquad \text{for } e_\ell > e_c \tag{A20a}$$

$$g_w = g_b \qquad \text{for } e_\ell \leq e_c \tag{A20b}$$

$$E_\ell = g_w[e_\ell - e_c]/P \tag{A21}$$

$$E_s + E_\ell - E = 0 \tag{A22}$$

$$H_\ell = \rho c_p g_{bH}(T_\ell - T_c) \tag{A23}$$

$$I_a + L_a - L_e - H_\ell - \lambda E_\ell = 0 \tag{A24}$$

where λ is the latent heat of vapourisation of water, which is a $f(T_\ell)$, and g_s is discussed in Model Parameterisation. Equation (A22) is solved iteratively to find e_c; all three of E, E_ℓ, and E_s are functions of e_c. Dew forms on the canopy (E_ℓ is negative) when $e_\ell < e_c$. Equation (A24) is used to find T_ℓ by iterative means; L_e, H_ℓ, λ, and E_ℓ are all functions of T_ℓ. Shortwave and longwave radiation absorption are static parameters, i.e. they are calculated only once during a time step.

Canopy airspace temperature T_c is found from an iterative solution of

$$H_s + H_\ell - H = 0. \tag{A25}$$

Mesophyll Carbon Metabolism and CO_2 Partial Pressures

Respiration, Photosynthesis and Photorespiration

Leaf respiration R_d is calculated as before (Amthor 1994*a*), although r_t is given by a slightly different equation

$$\Delta T = T_\ell - T_{acc} \tag{A26}$$

$$r_t = 433{\cdot}5 \times 10^6 \exp\left[-5830/(\Delta T + 293{\cdot}15)\right]/ \left[1 + \exp\left(T_\ell - 50 - 0{\cdot}15\, T_{acc}\right)\right] \tag{A27}$$

$$r_c = \exp\left[0{\cdot}0087\,(50 - C_i)\right] \tag{A28}$$

$$r_\ell = \max\left\{0{\cdot}6,\ 1 - 40000\,\Theta\right\} \tag{A29}$$

$$R_m = r_c r_\ell r_t m_r N \tag{A30}$$

$$R_d = R_m + R_g + l_r L_{load}\,, \tag{A31}$$

where Θ is PPFD incident on the canopy and $l_r L_{load}$ represents respiration supporting the energetic costs of phloem loading in leaves. The value of L_{load} is a function of source and sink activity, but was set to a constant (Table 1) in this test of the canopy model.

Leaf mesophyll photosynthesis P_s, photorespiration P_r, and net CO_2 exchange A_{net} are calculated with a form of the widely accepted biochemical model of Farquhar *et al.* (1980; see also Collatz *et al.* 1991). Some of the equations are discussed, and references are given, in Amthor (1994*a*), although the model has been modified slightly in the meantime

$$k_t = 2{\cdot}4^{0{\cdot}1\Delta T}/\left[1 + \exp\left(\left[84{\cdot}56\,(\Delta T + 298{\cdot}15) - 26460\right]/\left[\Delta T + 298{\cdot}15\right]\right)\right] \tag{A32}$$

$$V_{c(max)} = 0{\cdot}00125\, k_t\, k_{cat}\, f_{rub}\, N \tag{A33}$$

$$W_c = V_{c(max)} C_c/\left[C_c + K_c(1 + pO_2/K_o)\right] \tag{A34}$$

$$f_{PS} = f_{rub}^{0{\cdot}16} \tag{A35}$$

$$J = f_{PS}\Theta_a/2 \tag{A36}$$

$$\Gamma_* = 0{\cdot}5\, pO_2/\tau_{rub} \tag{A37}$$

$$W_j = J/(4 + 8\,\Gamma_*/C_c) \tag{A38}$$

$$\Phi = V_{c(max)}/8{\cdot}2 \tag{A39}$$

$$W_t = 3\Phi/(1 - \Gamma_*/C_c) \qquad \text{for } C_c > \Gamma_* \tag{A40a}$$

$$W_t = W_c \qquad \text{for } C_c \leq \Gamma_* \tag{A40b}$$

$$0{\cdot}96\,x^2 - (W_c + W_j)x + W_c W_j = 0 \tag{A41}$$

$$0{\cdot}98 V_c^2 - (x + W_t)V_c + x W_t = 0 \tag{A42}$$

$$P_s = (1 - \alpha_{ozone})V_c \tag{A43}$$

$$P_r = P_s \Gamma_*/C_c \tag{A44}$$

$$A_{net} = P_s - P_r - R_d\,, \tag{A45}$$

where x is an intermediate variable (see Collatz *et al.* 1991), the smaller root for x and V_c are used (equations A41 and A42), and 0·96 and 0·98 in equations (A41) and (A42) introduce colimitations on photosynthesis. Both k_t and r_t are unity at T_{acc}. As before, and based on Collatz *et al.* (1991), potential electron transport rate J is linearly related to PPFD absorbed by the canopy (Θ_a, mol m^{-2} s^{-1}). *Nota bene*: photosynthesis is based on chloroplast CO_2 partial pressure C_c rather than the intercellular CO_2 partial pressure C_i used in many models. Ozone uptake and its effect on photosynthesis, i.e., α_{ozone}, are described in Model Parameterisation.

Steady-state Carbon Dioxide Partial Pressures and Fluxes

Conductance of CO_2 from intercellular spaces to the chloroplast stroma (g_{chl}, mol CO_2 m^{-2} s^{-1}) is given as before (Amthor 1994*a*)

$$g_{chl} = V_{c(max)}/(200 \times 10^{-6} + V_{c(max)}) . \tag{A46}$$

Partial pressures of CO_2 within the leaf are given by

$$C_c = C_{can} - A_{net}P(1{\cdot}37/g_b + 1{\cdot}6/g_s + 1/g_{chl}) \tag{A47}$$

$$C_i = C_c + A_{net}P/g_{chl} . \tag{A48}$$

Flux of CO_2 through the horizontal plane at height z ($F(z)$, mol CO_2 m^{-2} s^{-1}) and the partial pressure of CO_2 in the canopy airspace C_{can} are given by

$$F(z) = g_{aW}(C_a - C_{can})/P \tag{A49}$$

$$R_{soil} + R_{stem} - A_{net} + F(z) = 0 \tag{A50}$$

where equation (A50) is solved iteratively for the steady-state value of $F(z)$ because A_{net} is a function of C_{can} (Table 3).

Manuscript received 13 December 1993, accepted 19 April 1994